esa ESRIN

eurimage

Earth Watching

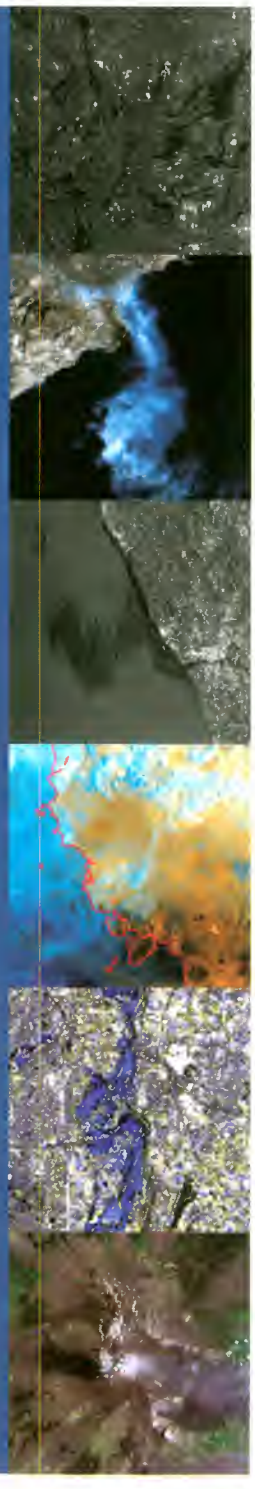

Anthology

European Space Agency
Agence spatiale européenne

EarthWatching

The Earth Watching project started at the end of 1993 during an emergency in Germany caused by serious floods that lasted for several days in the Cologne - Bonn area. We realised that during natural disasters, users and governmental authorities need data over the affected areas in very short timeframes – shorter than normal data delivery times – in order to co-ordinate rescue activities.

Thus Eurimage, in collaboration with the European Space Agency's (ESA) ESRIN facility, developed the Earth Watching service to help local authorities and to promote the benefits of remote sensing data during emergencies.

Satellite data can provide an overview of a situation quickly, as large areas can be covered in one pass, indicating zones already or probably affected and those in danger.

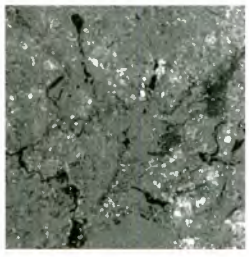

The radar missions, like ESA's ERS–1 and ERS–2 satellites, are excellent tools for monitoring areas in situations such as floods and oil spills. Thanks to its all-weather capability, it can acquire data independently of light or cloud coverage conditions.

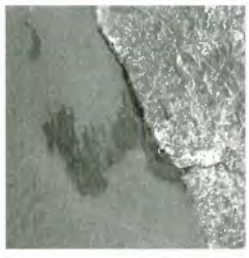

Optical missions, such as NOAA's AVHRR, the Russian RESURS-O1 and EOSAT's Landsat 5, are an excellent means of monitoring the fires that particularly affect the countries of the Mediterranean Basin during summer. The AVHRR and RESURS-O1 satellites, with their wide swath and high passage frequency, can be used for detecting medium to large fires, while Landsat 5 can can provide more precise details of already active fires and burned areas.

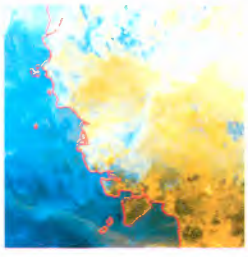

The Earth Watching project aims not only to show natural disasters, but also to promote various satellite remote sensing applications through images and articles for newspapers, magazines and TV stations.

To see the full range of Earth Watching data, visit our Website ...

http://earth.esa.int
http://www.eurimage.it

Earth Watching Structure

The small Earth Watching team operates on a best effort basis and, on receiving an alert, interrupts normal activities and start collecting information about the event through press agencies and throughout the Eurimage distributor network (around 40 distributors located in 32 countries in Europe, North Africa and the Middle East). A satellite acquisition plan is then prepared, as well as a fast data reception channel. Only one person is fully dedicated to this service,the main role of which is to test new techniques, filters, layouts and dissemination systems to offer a better and better service.

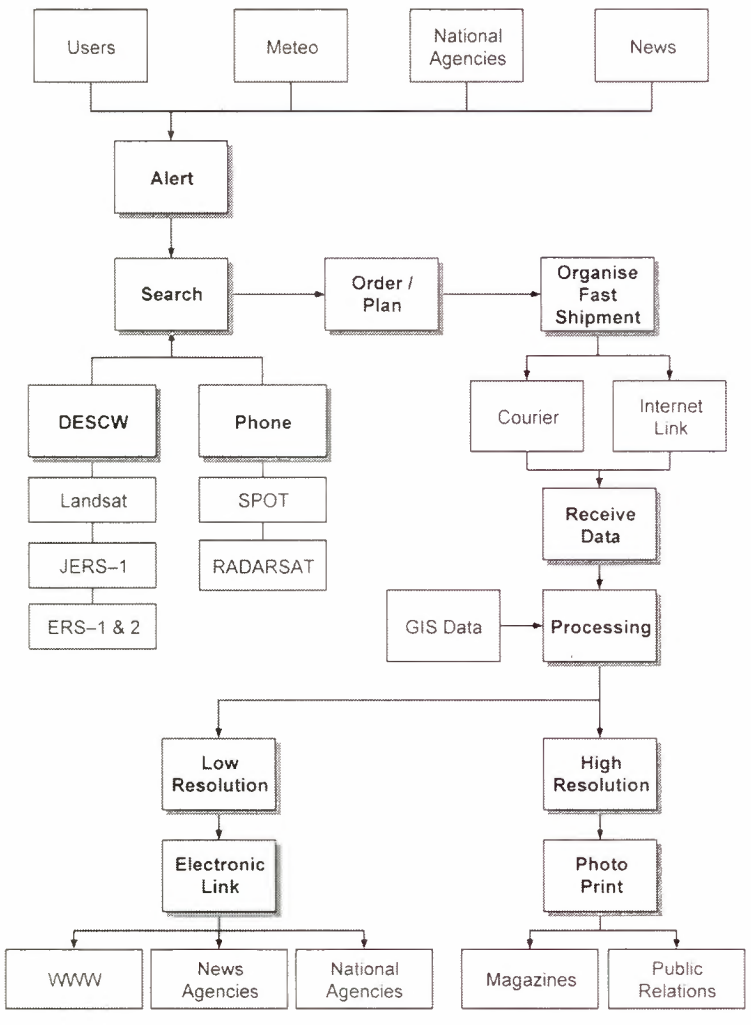

Earth Watching Information Flow

Through special delivery the data is received at the ESRIN processing facility a few hours after acquisition at the Ground Station and a full-resolution image is generated. From this, a low resolution version (whole or part of the image) is prepared and put on the Internet, where it is accessible through standard World Wide Web graphical browsers such as Netscape or Internet Explorer. Sometime it is more convenient to ask generation at a Ground Station of a low resolution image (called "Quick Look") that can be sent us by electronic link. This image can be available within 1-2 hours from acquisiton. When necessary the full resolution product is generated too. Prints of the images, also of high quality, are made available to Eurimage and ESA/ESRIN Public Relations for distribution to interested newspapers, magazine, or TV stations. Normally the team are able to produce an image within 5-6 hours of acquisition (full or low resolution, depending on the location and the links with the receiving ground station).

Often the Earth Watching Team co-operates with other research institutes or national entities to offer a better service or result. An example is the flooding in Bezier (F) during 1996. Something new is attempted at each event, in order to improve the readability of the images (radar images are not easily interpreted), for example superimposing GIS (Geographical Information System) information.

Fires

EVERY YEAR MILLIONS OF TONS of forest and savanna all over the world are destroyed and animal and plant species disappear as a result of deforestation and fires caused by human activity. A drastic reduction in forests has significant effects on the delicate global ecosystem.

During the last twenty years forest fires have increased in the Mediterranean countries, taking a heavy toll in lives and property. These countries are very vulnerable to fire because of the character of the Mediterranean scrub and the poor summer rainfall. The burned scrub needs 10-25 years to regrow, depending on the previous growth.

Areas burned in Greece, Italy, Portugal and Spain in the period 1980-1994.
Data Source: MIRAAF

Country		*Greece*	*Italy*	*Portugal*	*Spain*
No.of fires		1,712	12,935	19,100	13.261
Burned area (ha)	Forest	26,979	68,977	59,502	112,585
	Non-forest	16.917	83,989	36,312	129.450
Average fire area (ha)		15.08	5.06	3.01	8.05
Forest	Total (kha)	2.512	6.750	2,755	8.388
	% burned yearly	1.01	1.00	2.02	1.03
Forest & wooded land	Total (kha)	6.032	8.550	3.102	25.622
	% burned yearly	0.07	1.07	3.00	0.09

Natural causes triggering off fires are principally lightning and spontaneous combustion of dry vegetation, but in addition to these natural causes there are numerous arsons reported during the summer season. After a dry season the undergrowth is rich in dry biomass that represents a dangerous accumulation of combustible material. Abandoned crop fields can also be a risk to natural growth. Prevention and early warning are the only means of reducing the enormous cost incurred by fire damage.

How can we limit these disasters?

Using data from satellites, it is possible to obtain quickly a general overview of the situation over large areas of terrain, to monitor the emergency, identify risks, detect fires and, once the fire has been controlled, assess the damage by mapping the extent of the burned areas.

Advanced Very High Resolution Radiometer (AVHRR) data from the NOAA TIROS satellite can be a good monitoring tool: this satellite provides data twice in the morning and twice in the afternoon, each scene covers an area 3000 x 6000 km, offering a constant vision of the earth's surface. Over one thousand images of fires have been used to develop a semiautomatic fire detection algorithm based on the sensitivity of AVHRR's channel 3 (3.7 micrometers) to fire temperatures (400-1000 K), while the size of the AVHRR images makes it possible to operate a detection service at a continental scale.

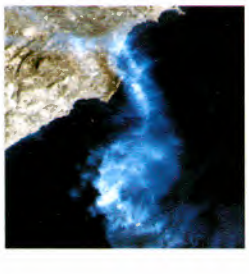

Landsat 5 with its Thematic Mapper (TM) instrument provides very impressive color images covering an area 180x180 km with 30 m of resolution, where it is possible to distinguish fire-damaged areas and active fires.

Both these optical satellites are able to detect fires and smoke.

Fires in Macao, Portugal, 1995

MACAO (PORTUGAL) JUNE '95 During the summer of 1995 many countries in Europe suffered fires that destroyed large areas of their Mediterranean scrub. The Landsat 5 satellite, with its Thematic Mapper instrument, is an excellent tool for viewing fires and can distinguish between areas already burned and active fires.

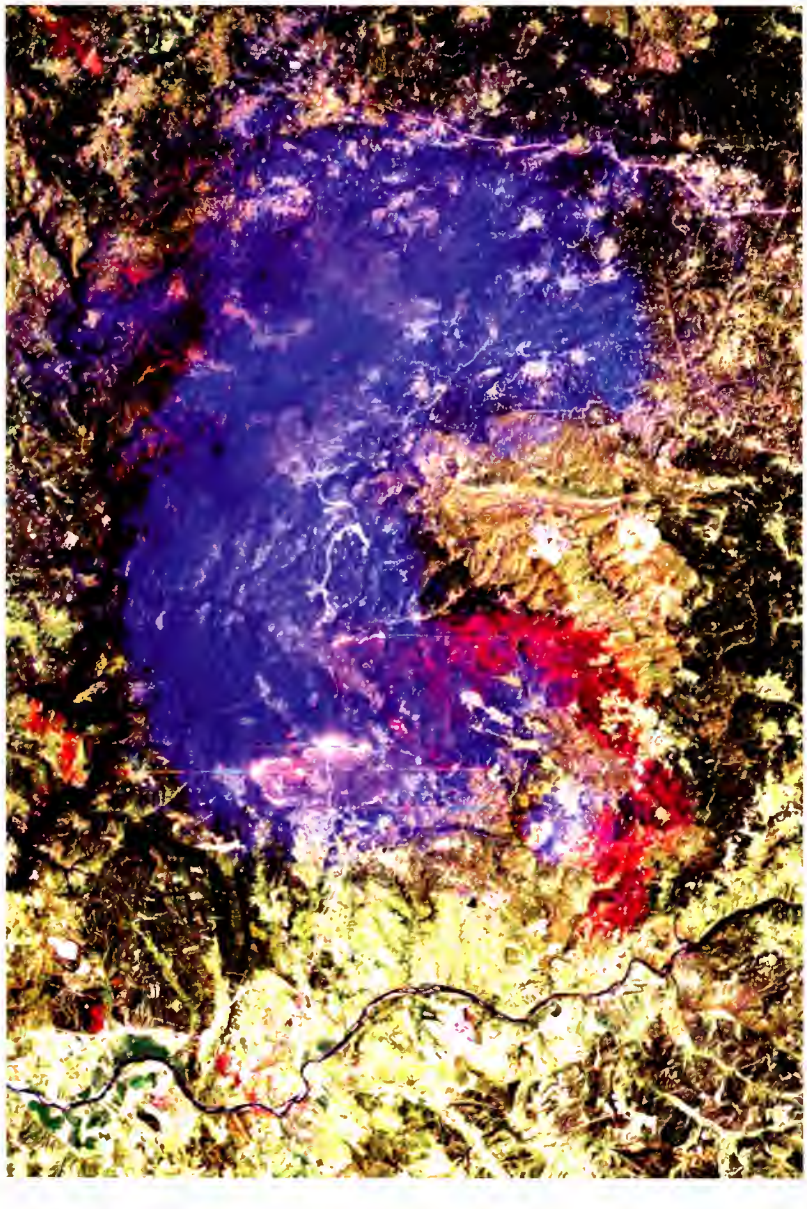

This scene of the Ribatejo region South East of the town of Coimbra, shows just a small part of the zone affected by the fires, focusing on the area where the fires were still active. The burnt area appears in dark reddish tones (the larger area in the central part of the image lies between the Tagus river to the South and the Zezere river to the West). The flames are shown by bright magenta and yellow saturated tones (the larger fire front is more than 5 Km long). The town of Macao is in the lower part of the image, on the right bank of the Tagus river, just inside the large burnt zone, and following the same river bank south, towards the lower corner of the image, the town of Abrantes can be seen. The selected band combination, 752, permits the discrimination of forests, rivers, urbanised areas and different soil types, making it possible to differentiate between areas burnt some days before the satellite acquisition and the zones where active fires are still burning. Band 2 is used to identify the dense smoke coming up from the fires.

Satellite / Sensor: Landsat 5 TM
Acquisition date: August 15th 1995
Track:203 - Row float 39.32N 07.46W
Acquired by: Fucino (Italy)

Fires & Smoke in S-E Asia, 1997

South-East Asia is suffering its worst drought in five decades and as a result, hundreds of forest fires - many deliberately started as method of clearing land, are burning out of control. A cloud of smoke covering an area more than half the size of the continental United States has sent the Air pollution index in the affected area well above the "hazardous" mark. In Sarawak (a main tourist spot in the Malaysian part of Borneo) the blanket of soot and smoke means that every man, woman and child are inhaling the equivalent of two and a half cigarettes a day. Without the seasonal monsoon rains to douse the fires, this could be one of the worst environmental disasters of the decade.

Borneo (Indonesia and Malaysia), is the third largest island in the world, with mountainous peaks of 900m to 2300m. It has a tropical climate with extreme humidity in the South of the island giving rise to luxuriant vegetation. The exceptionally dry weather conditions in 1997 caused large fires over all the plains.

Sumatra (Indonesia); the images cover the center and south part of the island. The fires are mainly located in the Lampung region (where the word 'Sumatra' appears on the map) and east of the town of Palembang (on the East coast). The Barisan Mountains chain traverses the Sumatra island, following the Western coast.

The team produced images from different ERS sensors. The following were derived from ATSR-2 (Along Track Scanning Radiometer) IRR data (nadir view), acquired over Indonesia during day and night ERS-2 satellite overpasses.

This images are compared to pictures derived from ERS-2 GOME (Global Ozone Monitoring Experiment) Level 2 products, which contain the total column amount of the trace gas nitrogen dioxide.

The ATSR Infrared instrument is a passive dual view (nadir and forward) self-calibrating radiometer which scans the Earth at a spatial resolution of 1 km on a 512 km swath. The ATSR-2 IRR has four infrared channels at 1.6 micron, 3.7 micron, 11 micron and 12 micron, and 3 visible channels at 0.55 micron, 0.65 micron 0.86 micron. The instrument is able to detect "hot" features relevant to the current fire activity.

GOME is a nadir scanning UV and visible spectrometer for global monitoring of ozone and other trace gases. Since July 1996 Level 2 products (total column amount of ozone and nitrogen dioxide operationally generated at D-PAF) are available to users. Nitrogen dioxide measurements can be used to monitor bio-mass burning. The GOME instrument can only measure during daytime. The swath consists of 3 groundpixels each having the size of 40 km along track and 320 km across track. To compare the GOME nitrogen dioxide measurements to ATSR-2 day measurements only the groundpixel in nadir was used to give similar coverage to the ATSR-2 instrument.

Borneo – Day time images

Day time images are derived by a RGB combination of 1.6 micron and 11 micron data showing reflective and thermal features which allow the visualisation of warmer clouds and fogs over land.

The data are at full 1 km resolution in satellite projection with image samples along satellite track, and image lines across satellite track .

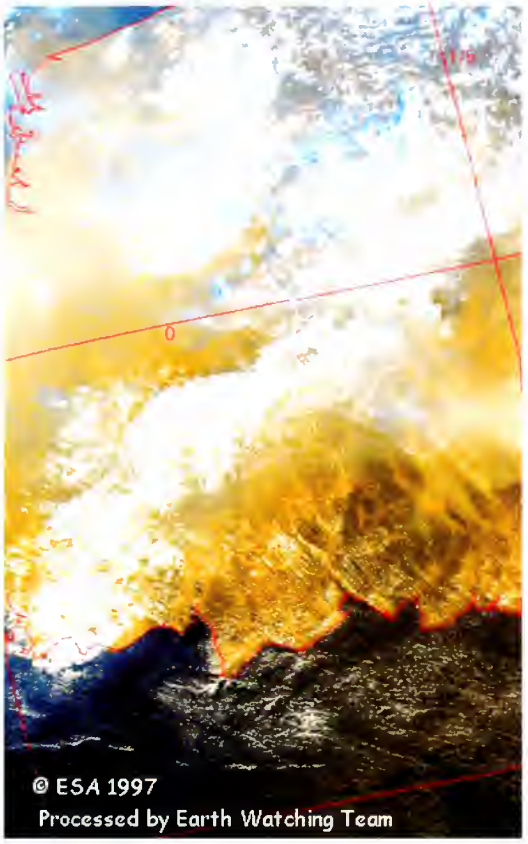

Dense fog visible in N, N-W and S-E part of the image. Smoke features in the S-E are also apparent. The fires are located in the Kalimantan Tengah region near the coastline. The town of Banjarmasin is located along the Barito river near the coast at the right border of the image.

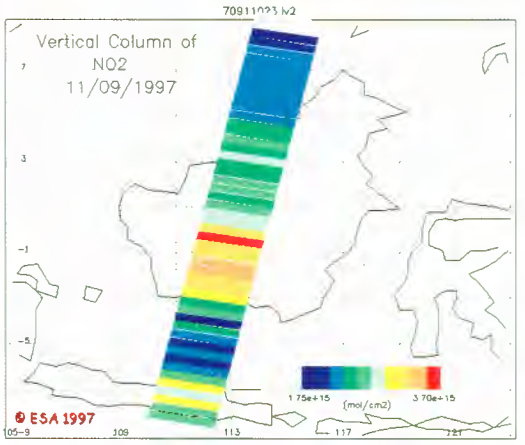

11th September 1997 - GOME instrument High values (yellow - red) indicate the areas of burning bio-mass.

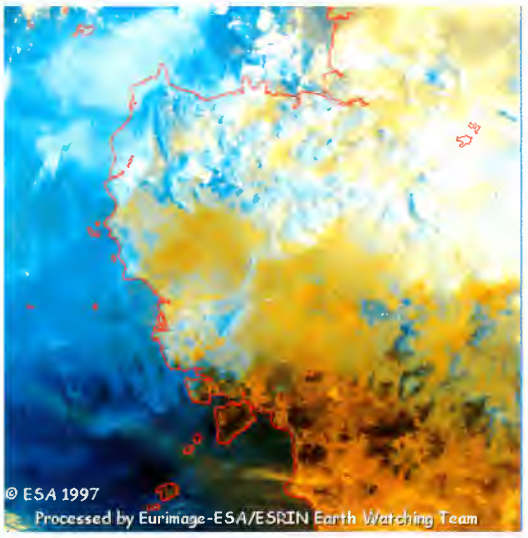

17th September 1997 - Day time image. The smoke plume is quite evident in the SE in coincidence with 15 September night image hot spots.

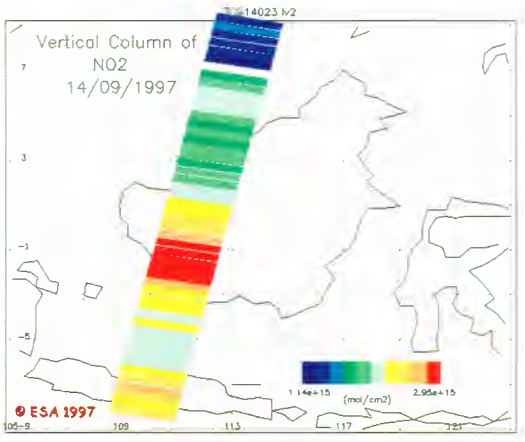

17th September 1997 - GOME instrument.

Analysis of bio-mass burning performed at DLR and the University of Bremen using GOME data.

Borneo – Night Images

Thse night images are derived from ATSR nadir view calibrated data. Many more examples are available on the Earth Watching Website. The RGB colour composition is made using 3.7 and 11 micro channels. In all the images, except the first one, all pixels showing saturation in the 3.7 micron channel (temperature above 312 K (39 C) degrees) have been superimposed on the final RGB composite as red "hot" spots. The cold clouds with temperatures less than 274 K (1 C) in both channels appear in black color in the images. The warmer areas with temperature greater than 305 K (32 C) in channel 3.7 appear as clear yellow features . The Coastlines have been set over images in white color to evidence Land/Sea contours. The data are at full resolution (1km) in satellite projection with image samples along satellite track and image lines across satellite track.

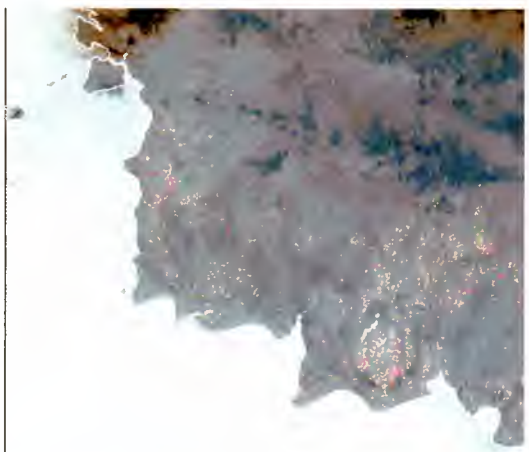

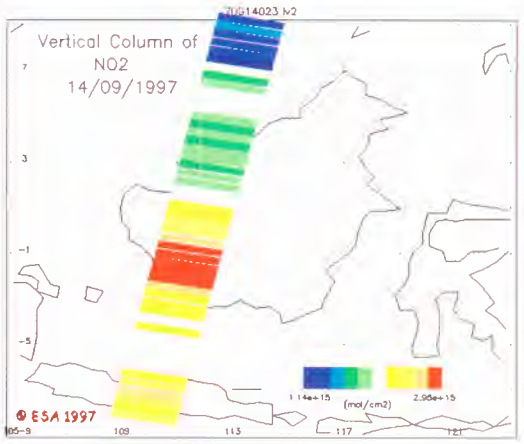

ATSR: 15/9/97 *GOME: 14/9/97*

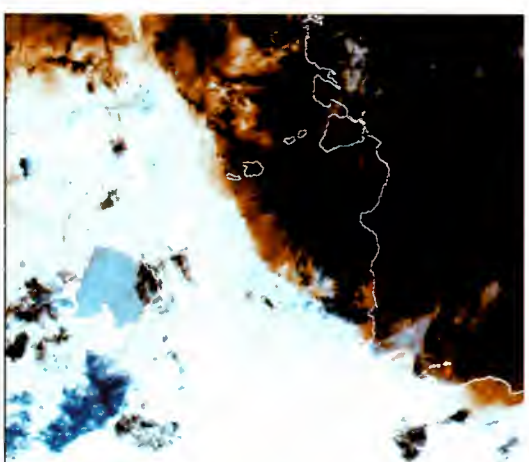

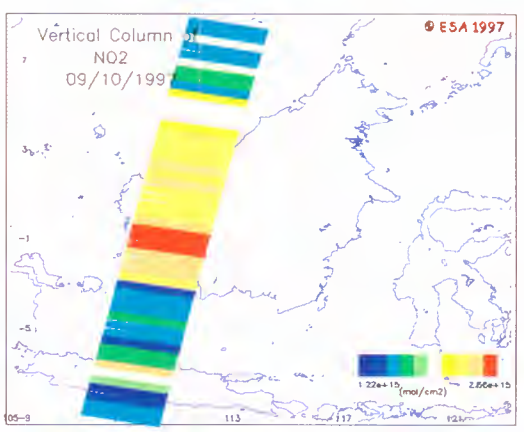

ATSR: 7/10/97 *GOME: 9/10/97*

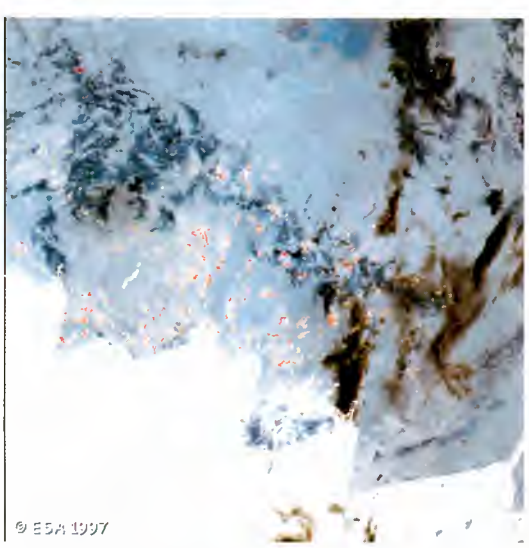

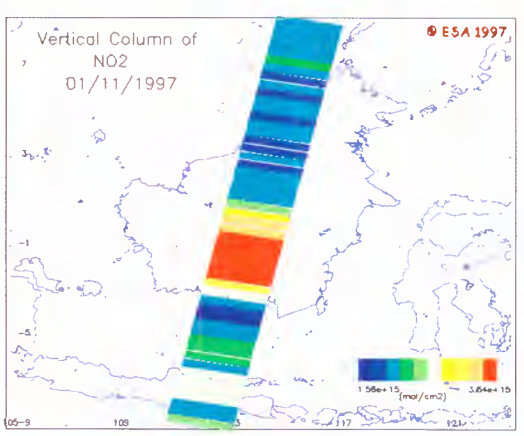

ATSR: 30/10/97 *GOME: 1/11/97*

To demonstrate the possibility of measuring bio-mass burning with the GOME instrument and to show a possible synergy between GOME and ATSR, the following steps were performed: - GOME products were selected with a maximum time difference to the ATSR data of one day - out of the three GOME groundpixels (total swath of 960 km) the pixel was used which corresponds best to the ATSR coverage High values in the GOME nitrogen dioxide measurements can be directly compared to the ATSR "fire measurements" and indicate very well the bio-mass of burning areas.

Borneo – ERS SAR Multi-temporal Image

This SAR image shows an area that cover the eastern part of the Tanjung Puting National Park, the largest and most diverse protected example of the extensive coastal tropical heath and peat swamp forest which used to cover much of southern Borneo. The park contains 3.040 sq km of low lying swampy terrain punctuated by blackwater rivers which flow into the Java Sea. The best known animals in Tanjung Puting are the orangutans and the bizarre looking proboscis monkey with its "Jimmy Durante" nose as well as seven other primate species. Clouded leopards, civets, and Malaysian sun bears live in the park as do mouse deer. barking deer. sambar deer, the wild cattle known as banteng and over 220 species of birds.

In the multitemporal image. yellow-orange colours show the healthy vegetation. while the areas appearing in magenta tones are probably the ones affected by the deforestation caused by the fires.

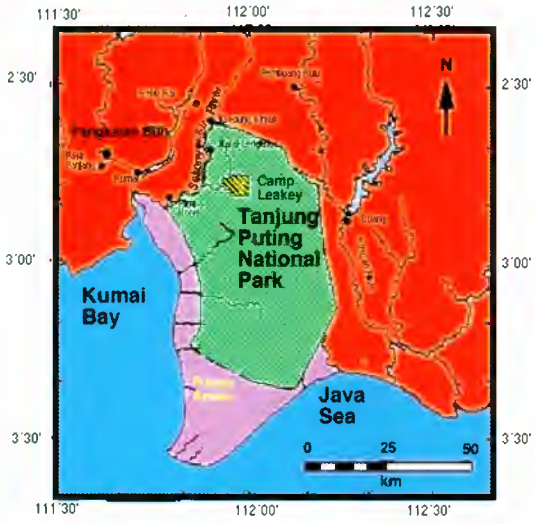

Map of Tanjung Puting National Park

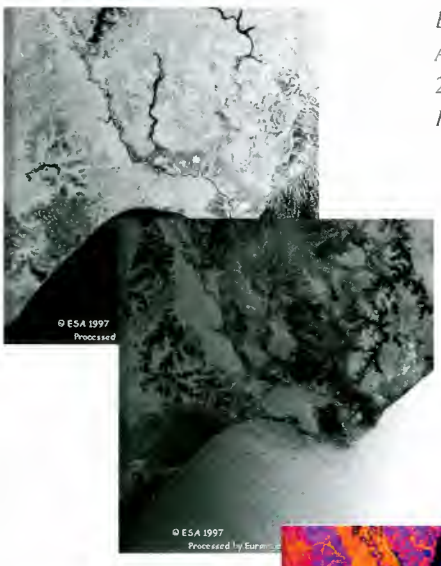

ERS/2 SAR
Acquisition date
25/10/96: Orbit 7916
Frame: 3672

ERS/2 SAR
Acquisition date
10/10/97: Orbit 12926
Frame: 3672

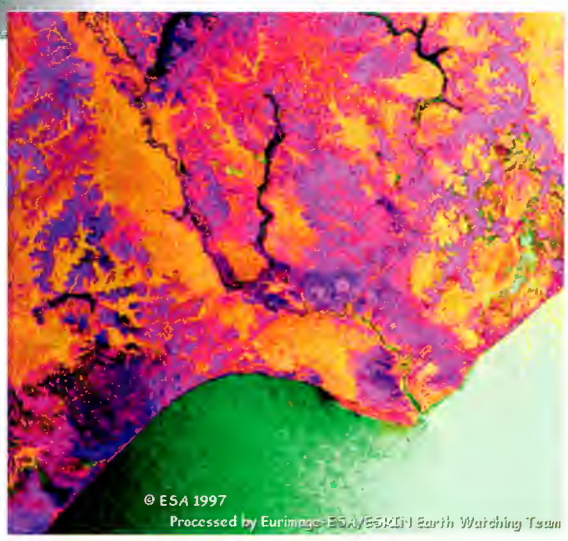

ERS/2 SAR
Multitemporal Image

Borneo – 1998

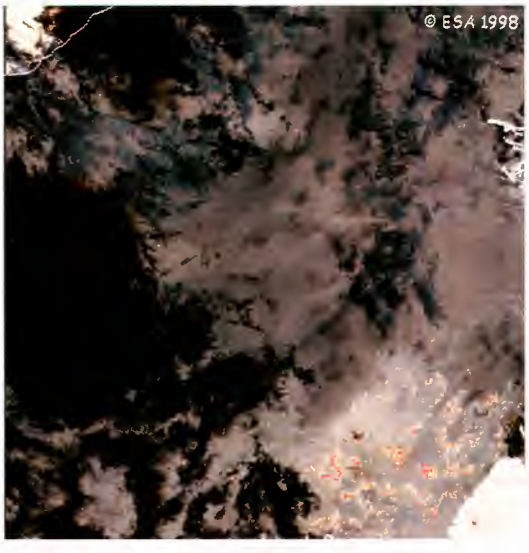

16/3/98

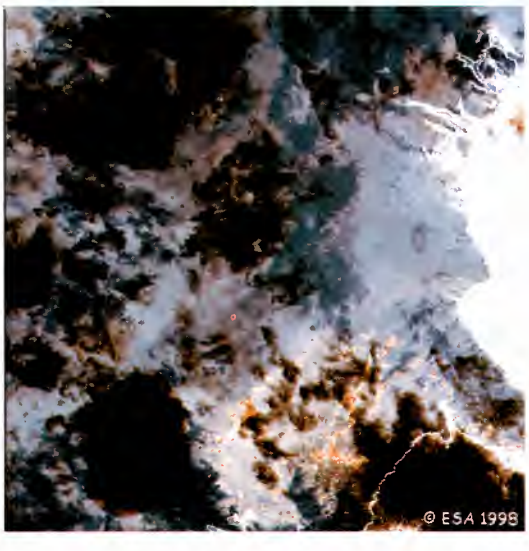

1/4/98

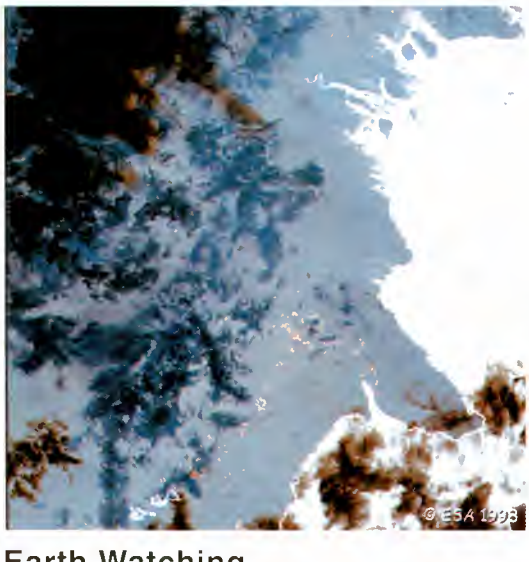

17/4/98

In December 1997, seasonal rains seemed to have put an end to the fires in Indonesia which by then had caused more than 1.3 billion dollars in damage, but by the end of January they were burning again.

The economic crisis in South-East Asia, added to the threat, with fewer resources available for fighting the fires, and more pressure on people to set them to clear land and raise income.

In East Kalimantan on the island of Borneo, the new fires threatened large parts of the natural habitat of the orangutan, already under threat from poachers and human encroachment. Fewer than 25,000 are believed to survive in the wild.

These ATSR night images show the progress of fires in East Borneo in March and April

Fires in Central America, 1998

Throughout the spring of 1998, Central America was devastated by forest fires. By the middle of May Mexico had already had over 9,000 forest fires — 87% more than the previous year — and some 250,000 hectares of forest had been affected. 19 Firefighters died in a single incident in Texocuixpan, 140 km east of Mexico City, and smoke from the fires closed schools and airports as far away as Texas.

The fires were blamed on drought triggered by El Nino, on careless farmers clearing land for planting, and on deliberate arson to clear land for construction or for the cultivation of marijuana and opium.

These night time images are derived from ATSR nadir view calibrated data. The RGB colour composition is made using 3.7 and 11 micro channels. All pixels showing saturation in the 3.7 micron channel (temperature above 312 K (39° C) degrees) have been superimposed on the final RGB composite as red "hot" spots. The cold clouds with temperatures less than 274 K (1° C) in both channels appear in black color in the images. The warmer areas with temperature greater than 305 K (32 C) in channel 3.7 appear as clear yellow features. These images are composites and show small variations in colour between different parts of the image.

18/--4/98

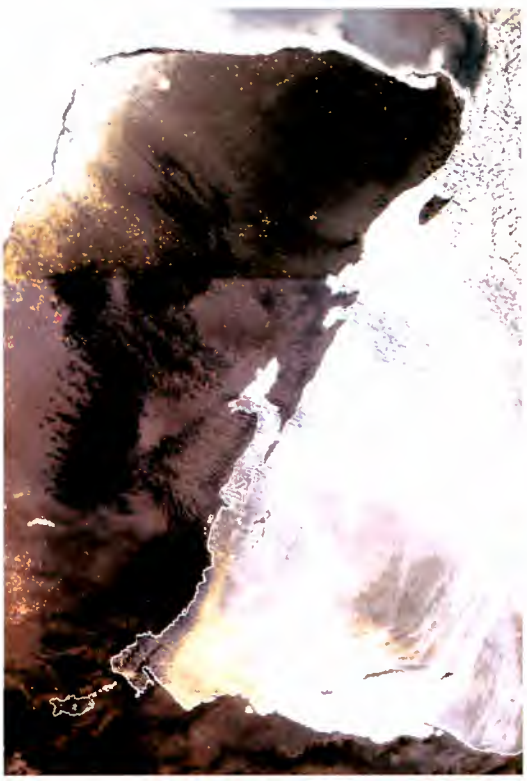

17/3/98

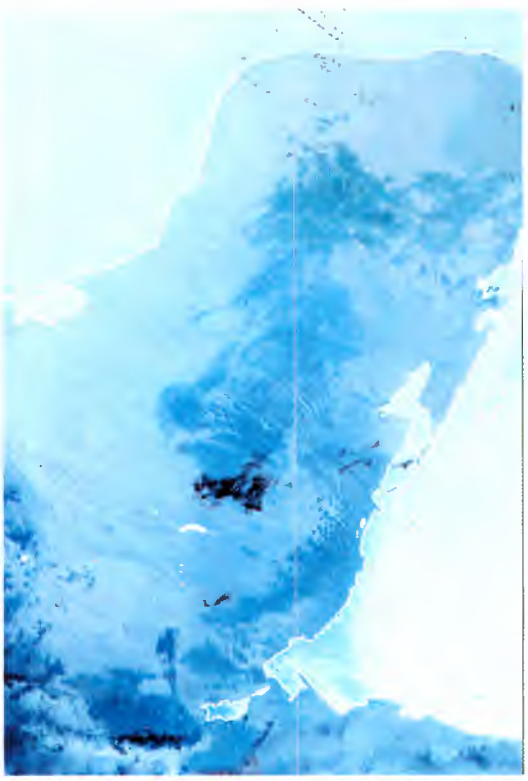

Fires in Central America, 1998

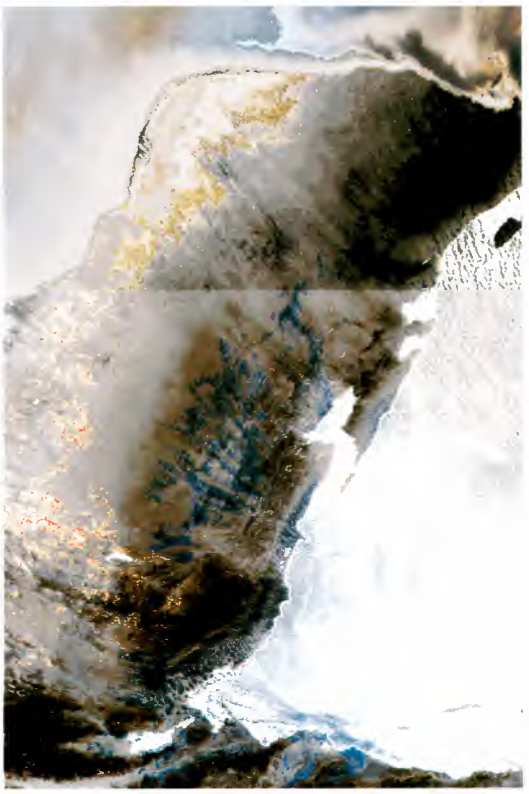

7/5/98

In parts of Mexico visibility dropped to less than two kilometres. The Mexican Environment Ministry admits that it is unable to prevent the fires, or to do much about putting them out.

By the end of May, some rain had fallen, but most of the fires were continuing to burn. Emergency measures introduced to limit pollution in Mexico City were estimated as costing 30 million dollars a day in lost earnings, while ranchers were forced to slaughter animals before they died of starvation and thirst.

10/5/98

Fires - Summer 1998
ATSR fire monitoring over Europe

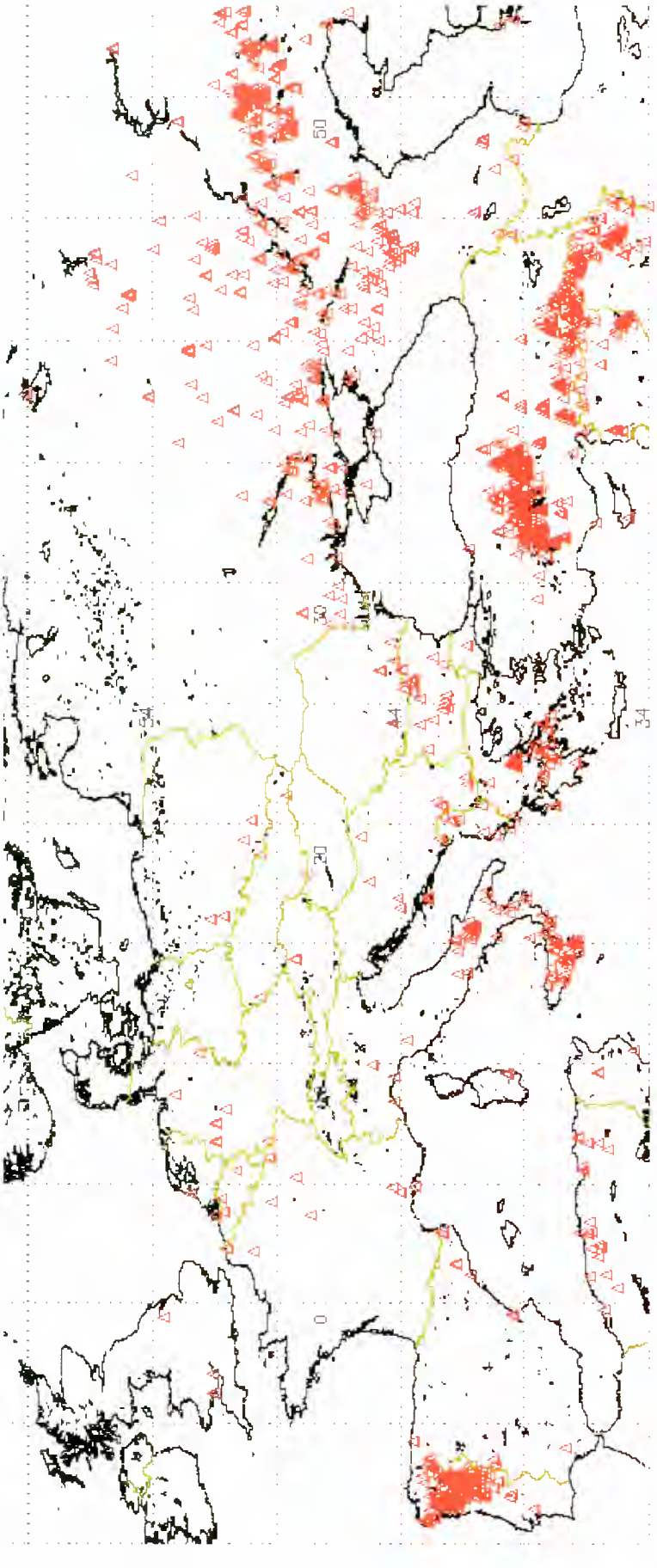

THE IMAGE SHOWS a collection of "hot spots" detected over Europe and the Middle East during the period 1st June - 31st August 1998. They were derived from ATSR-2 Rush Fire products, generated from data acquired using ERS-2 satellite night time overpasses.

All images (2069) collected over Europe during the above period, were analysed in order to pick up 4794 "hot spots". The results are available to the user Community on the Internet web site:

http://shark1.esrin.esa.it.

Foreseen delivery of the NRT (Near Real Time) processing system in Tromsoe may allow to have this information available to users within 2/3 hours from sensing.

The image clearly shows high distribution of fires over Portugal, South of Italy, Greece, Turkey and Caucasian regions. The "hot spots" on the Caspian Sea and over the Middle East are thought to be mainly caused by oil drilling facilities located in those regions. The "hot spot" detection activity demonstrates the capabilities of the ATSR for applications in fire statistics and fire monitoring. Further more it will provide sound experience and knowledge for the future ESA Earth Watch missions.

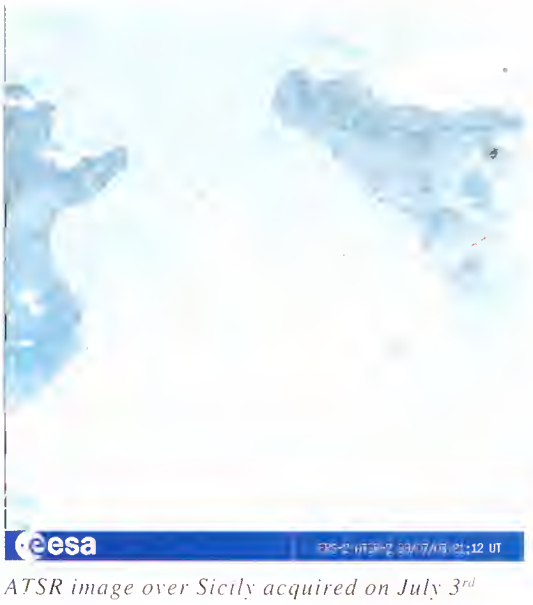

ATSR image over Sicily acquired on July 3rd

4794 Hot Spots detected in 2096 ATSR-2 night time overpasses

Floods

EACH YEAR HEAVY RAIN severely affects the Earth causing considerable damage to towns, roads and agriculture with a high loss of life. One of the biggest problems during these emergencies is to obtain an overall view of the phenomenon, with a clear idea of the extent of the flooded area, and, to predict the likely developments. Aerial observation is often impossible due to prohibitive weather conditions and, if the phenomenon is widespread, would be very time-consuming and expensive. Many of the world's urban centres are in low-lying areas subject to flooding, and rapid identification and response to flooding is essential to avoid turning an environmental phenomenon into a potentially grave disaster.

After the floods have subsided, a more precise assessment of the damaged area is needed by authorities and by insurance companies providing cover against natural hazards. Detailed maps of the event are necessary for both hazard assessment and as input to hydrological models used to plan structural alteration of watercourses. The extent to which remote sensing data are can be successfully used in flood monitoring is still widely unexploited. Potential users are not familiar with the procedure for obtaining satellite data and processing and interpreting the images. The European Space Agency's ERS-1 and ERS-2 satellites carry a Synthetic Aperture Radar (SAR) instrument, which can collect data independently of weather and light conditions: it is an excellent choice for tracking the catastrophic winter floods that occur each year in Europe, particulary since the weather during these periods is always overcast and rainy.

To better show the flooded areas a multitemporal technique is normally used to identify and highlight the flooded areas. This technique uses black and white radar images of the same area taken on different dates and assigns them to the red, green and blue colour channels in a colour image. The resulting multitemporal image clearly reveals change in the Earth's surface by the presence of colour in the image: the hue of the colour indicating the date of the change and the intensity of the colour the degree of change. Many of these techniques require the use of a reference image from the archive, showing the "normal" situation. Strangely these can sometimes take longer to arrive than the freshly acquired data, as the data are stored unprocessed in various Processing and Archiving Facilities (PAFs) and some time is needed to retrieve and process the data.

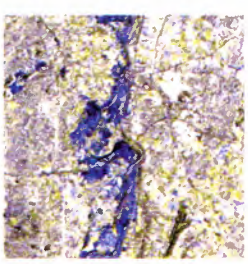

Floods – The Netherlands, 1995

THE HEAVY RAIN THAT HIT FRANCE (in the area of Charleville) and Germany at the end of January '95 enlarged the Mass (Meuse), Waal and Rhine rivers, threatening to overwhelm the Netherlands' flood protection walls and inundate the heart of the country.

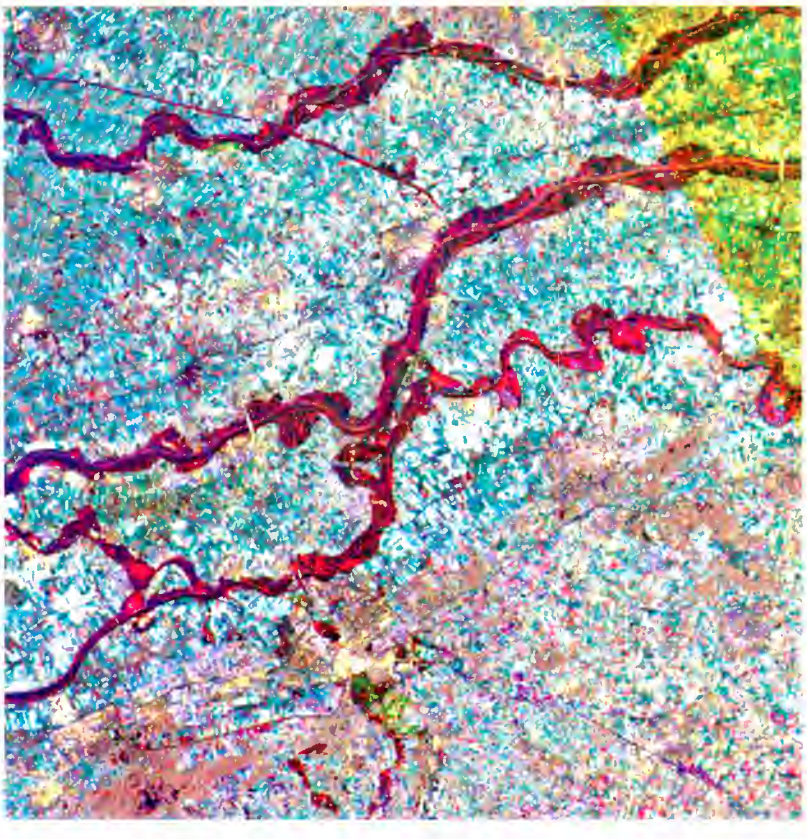

The Earth Watching team, observing the flood's critical high point move down the Maas river, processed image after image, including this multitemporal image of the Nijmegen area.

The image shows the three rivers, the Lower Rhine (top), the Waals (centre) and the Maas (bottom) in an area just west of the town of Nijmegen. The scene covers 45 km by 60 km, with the city of Hertogenbosh near the centre and Tilburg towards the lower left corner.

The multitemporal display shows the situation between the 30th January 1995 (green) and 5th February 5 (red) in comparison with the normal situation during the previous autumn (21th September 1994, displayed in blue). The swollen rivers are well delineated here in darker red, while the normal river courses can be identified by black lines or as two parallel lines indicating the banks.

The urban area appears in cyan, with some red spots. This can be explained by the change in radar-illumination, since the ascending orbit (5th February), E-NE looking, has been combined with two descending passes, looking W-SW.

The magenta patches in these areas show the results of the flooding on the 5th of February, whilst the dark green in the rest of the image indicates where flooding occurred between the 30th and the 5th. The greenish and yellowish tones throughout the image show that on both dates, but specially the 30th, it was wetter than on the autumn acquisition date.

Note that the area in the top left is covered only by the descending orbits; hence, the red colour component is missing, giving this yellow colour. The wooded area is shown in a homogeneous grey-bluish tone.

ERS-1 SAR
Red: February 5th, 1995; Green: January 30th, 1995; Blue: September 21th, 1994
Orbits: 18624, Frame 1035
Orbits: 18531, 16651 Frame 2565,
Acquired by Fucino (Italy)

The Netherlands, February 1995

Maastricht

The heavy rainfall at the end of January 95, together with the snow melt in the Alps, caused extensive flooding along the Maas (or Meuse) river.

On the 25 January the water level of the Maas river started rising dangerously in the South of the Netherlands, near the town of Maastricht. On 30 January the Government of The Netherlands decided to evacuate about 75,000 inhabitants living along the Maas and the Waal.

This SAR (Synthetic Aperture Radar) image represents the region of Maastricht, Netherlands. The Maas (or Meuse) river flows from the bottom to the upper part of the image showing the boundary line between Belgium (left) and the Netherlands (right).

The colours in the image are achieved by merging the two data sets assigning a blue colour to the September acquisition and yellow colour to the second one. This makes it possible to visualise clearly all the changes between the two acquisition dates.

The most significant changes are marked in blue showing the flooding areas. They are located mainly along the Maas river, representing a total surface within the image of 3520 hectares.

Near the middle of the picture, just south of the large flooded areas, lies the city of Maastricht, shown by bright points.

A canal (in black - dark blue), starting south of Maastricht and flowing west, near the city of Genk (Belgium) is also clearly visible in the image.

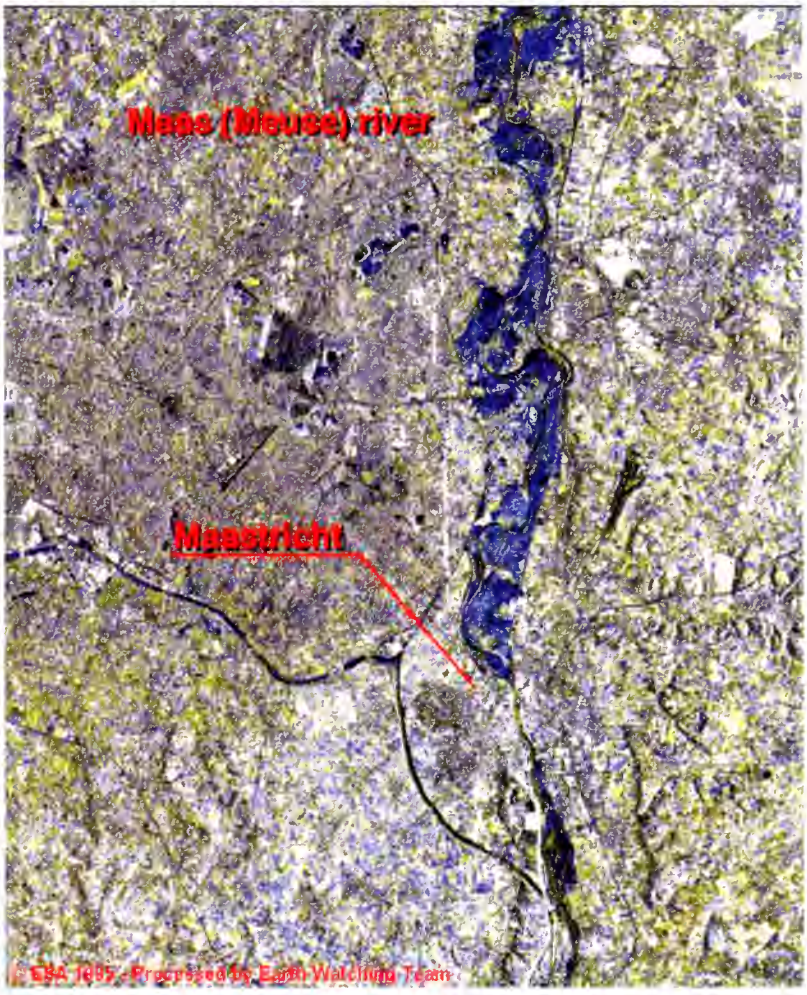

ERS-1 SAR
Red: January 30th, 1995
Green: January 30th, 1995
Blue: September 21th, 1994
Orbits: 18531, 16651
Frame 2583
Acquired by Fucino (Italy)

Floods – Beziers, France, 1996

On January 29, 1996, in the dark of night, at lightning speed, a large flood descended on the small southern French town of Beziers. It only took a few hours of torrential rain for the nearby Orb river to overflow, claiming four lives. More than six hundred people were evacuated. From the Loire to the Ardennes, 2700 towns and villages were left in a state of disaster. Eurimage's Earth Watching team was ready to respond, and brought the images to the Web within days of the flood.

ERS-1 passed over at 23.00 local time on the 28th January 1996, during heavy rainfall (more than 200 mm in 24 Hrs); ERS-2 crossed the area at the same time, but one day later when the flooding was still high. This multitemporal image, obtained by merging data from both satellites, shows the bright spots of the city of Beziers and towards the left bottom the city of Narbonne. Due to very wet soil conditions on both dates, the prevailing colour in the coastal plain is greenish-cyan, except for the hills of Montagne de la Clape, covered with Mediterranean shrubs and pines.

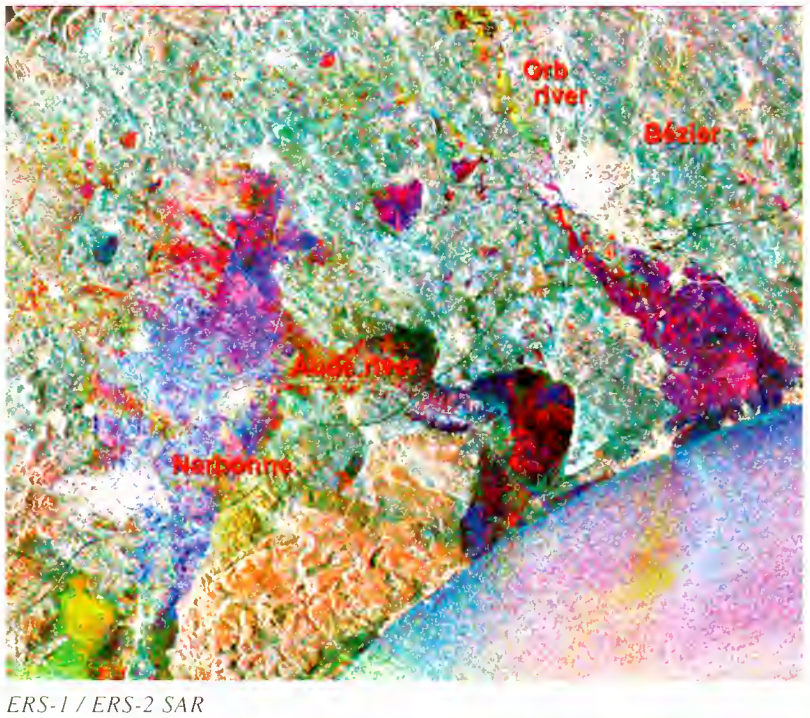

ERS-1 / ERS-2 SAR
Red: ERS-2 7/8/95
Green: ERS-2 29/1/96
Blue: ERS-1 28/1/96
Orbits: ERS-2 1558, ERS-2 4063, ERS-1 23736
Frame 855
Acquired by: Fucino

The reddish zones and spots in the lower parts of the plain, (mainly composed of agricultural areas and ponds), were flooded during both January acquisitions. This flooding came from the river Aude, North and East of Narbonne. The worst damage occurred along the river Orb, crossing the city of Beziers. The green/yellowish area north of Beziers means that it was flooded on the 28th, and indicates the arrival of the water that has fallen as rain upstream in the mountains to the north. The huge bluish/magenta area to the south of Beziers and in other parts of the scene, as well as the reddish parts in the lowlands, reflect the situation of the flooded surface on the 29th. The large oblong area of a faint bluish colour appearing close to Narbonne still needs to be explained. It might be the strong backscatter of land hit by heavy rainfall immediately before and during the acquisition, leaving behind water soaked terrain.

When integrated in a GIS with other data having an impact on flooding mechanisms, this type of image is of great benefit for the estimation extent of the flood, as well as for the study of the flood dynamics over 24 hrs. Apart from this 'near real-time' use of ERS SAR, the data can also be used for the validation of hydrological models for assessing flood risks.

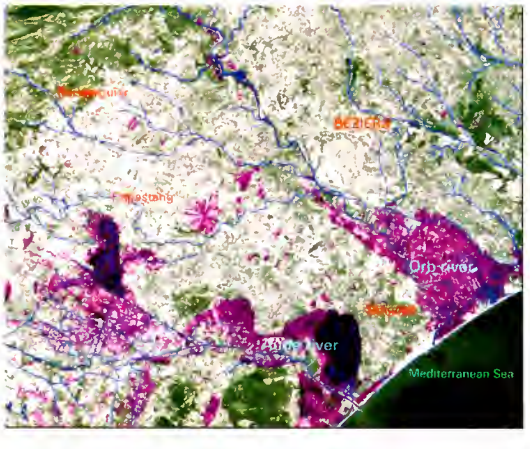

After the event the Laboratoire Commun de Teledetection CEMAGREF extracted from the above multitemporal SAR image the flooded areas and superimposed them on a SPOT pancromathic image.

Floods – Summer 1997

Austria, Czech Republic, Poland & Germany

RAIN CAUSED FLOODS in a third of the Poland countryside – the worst flooding in decades in the Czech Republic and Poland – destroying farmland and killing at least 52 people in Poland and 39 in the Czech Republic. In Poland, 300 towns and villages are under water. In the Czech Republic, the government said nearly 2,700 homes were destroyed by the flooding. Thousands of Czech and Polish people had to be evacuated after 10 July.

Hundreds of thousands of Czechs and Germans braced for a second wave of flooding on 21 July as falling rain continued to fuel the worst natural disaster to hit Central Europe in centuries and estimates were that the damage may have run as high as $2 billion. Such a natural disaster is very unusual in this region, so they were totally unprepared, with no tools to fight with floodwater. More than 10% of Polish territory was under water.

Despite massive reinforcement efforts and sandbagging, a third dike along the German portion of the Oder River (north the town of Frankfurt an der Oder) gave way on the 27 July, sending waters swirling up to roof height.

Map of area of Austria, Czech Republic, Poland & Germany affected by flooding, Summer 1997

Flooding – Summer 1997
Austria, Czech Republic, Poland & Germany

The ERS-2 Satellite covered the whole course of the Oder and Morava rivers twice during the flooding event. The satellite took the images westwards, following the flow of the Oder river. Each strip is 100 Km wide giving an overall overview of the phenomenon. In this mosaic what appears in black is water. The enlargement of the Oder river at several points is very evident: the larger one is located in correspondance of the town of Frankfurt ober Oder, located east of Berlin (the large, very bright area in the western strip).

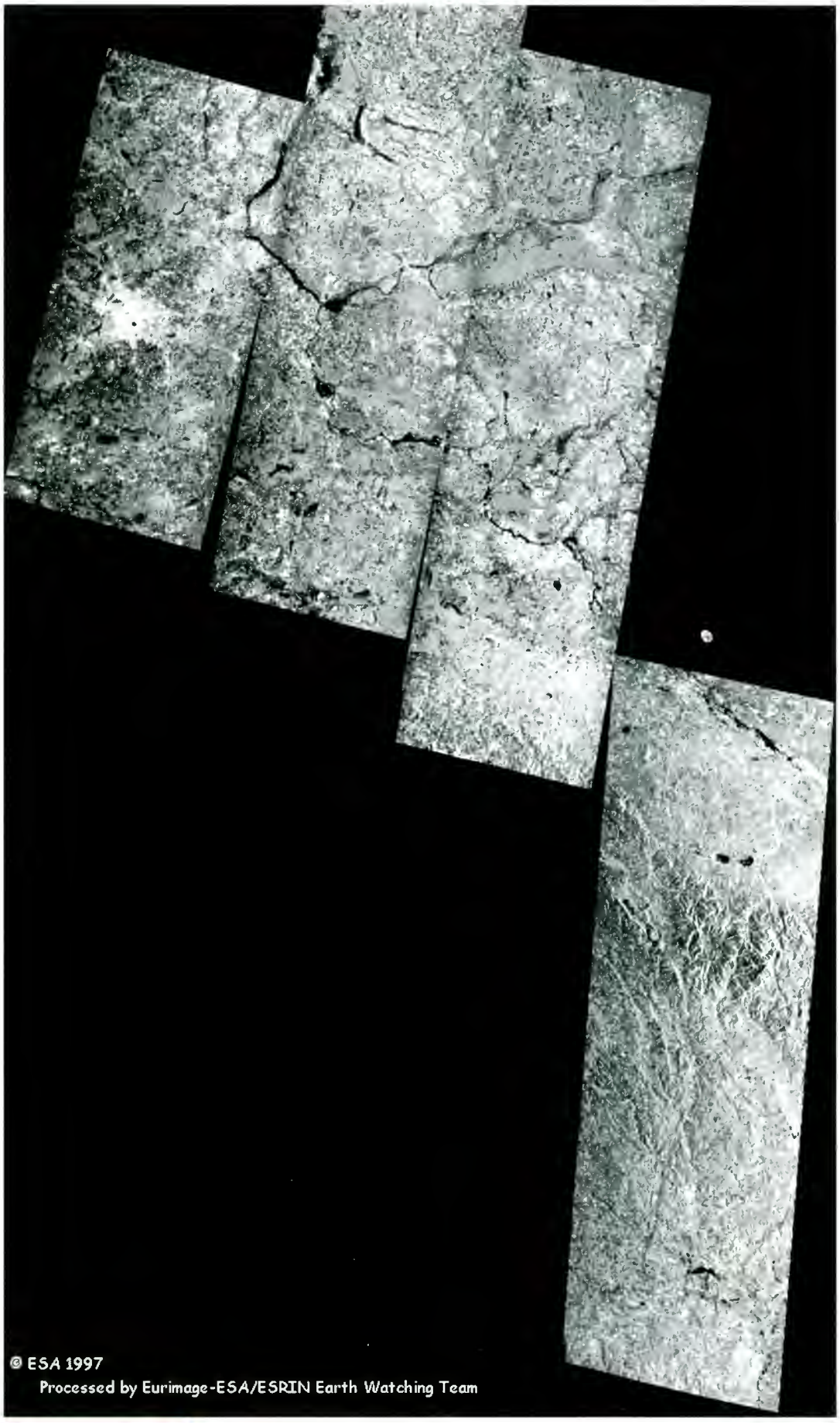

ERS SAR mosaic, from 30/7/07 to 9/8/97

Flooding – Summer 1997
Austria, Czech Republic, Poland & Germany

Plot of acquisitions of Landsat 5, ERS–1 & 2 SAR, JERS–1 VNIR over flooded areas in Austria, Czech Republic, Poland and Germany, July, August 1997

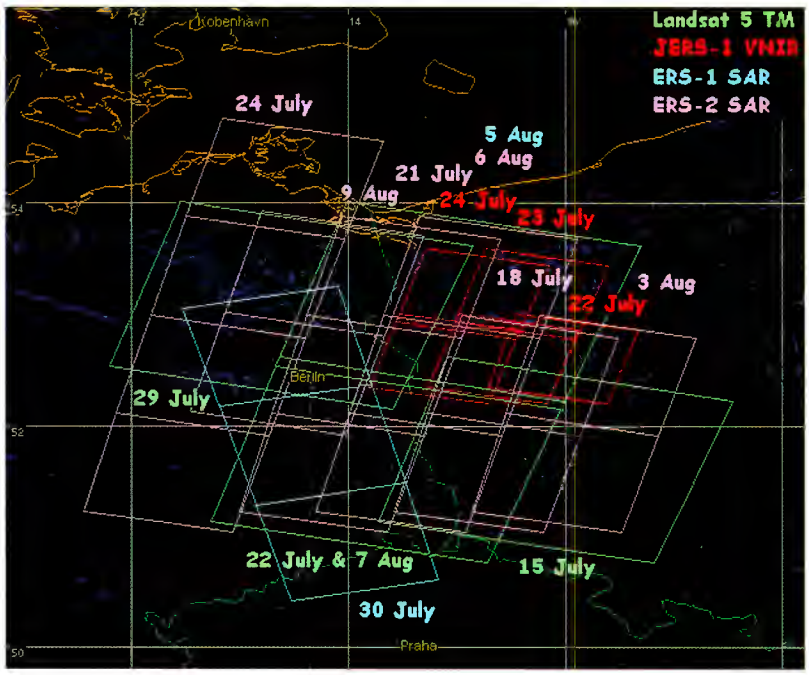

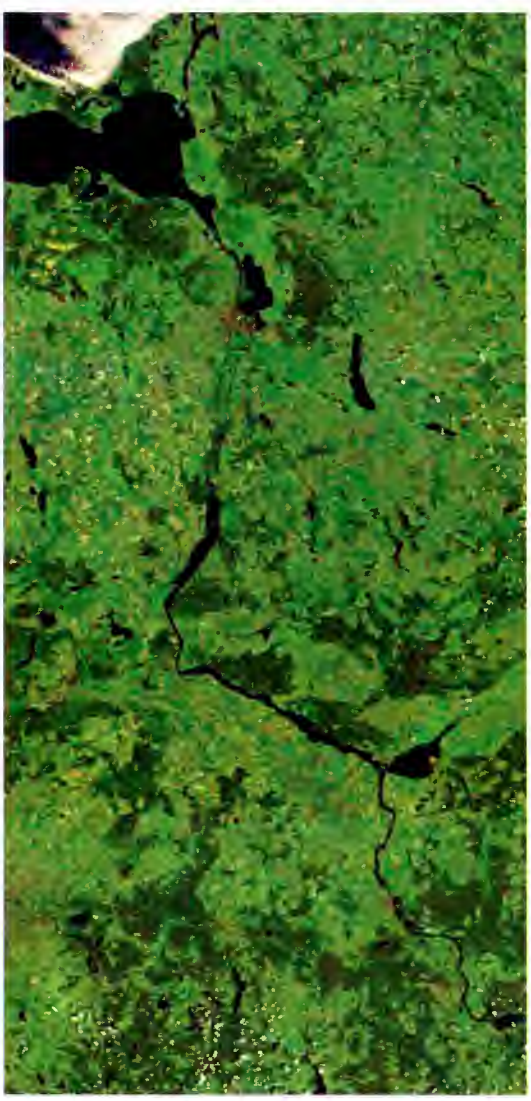

Landsat 5 TM
Bands 752 (RGB)
July 22nd, 1997
Track: 191; Frame: 24
Acquired by: Fucino
This Landsat 5 image shows the Oder river between the towns of Stettin and Frankfurt an der Oder. Dark, flooded areas are located at the confluence between the Oder and Warta rivers. The Eastern part of the town of Berlin is partially visible at the left edge of the image (near the bottom).

ERS-2 SAR
July 21st, 1997
Orbit: 11771
Frames: 2529–2565

Flooding – Summer 1997
Austria, Czech Republic, Poland & Germany

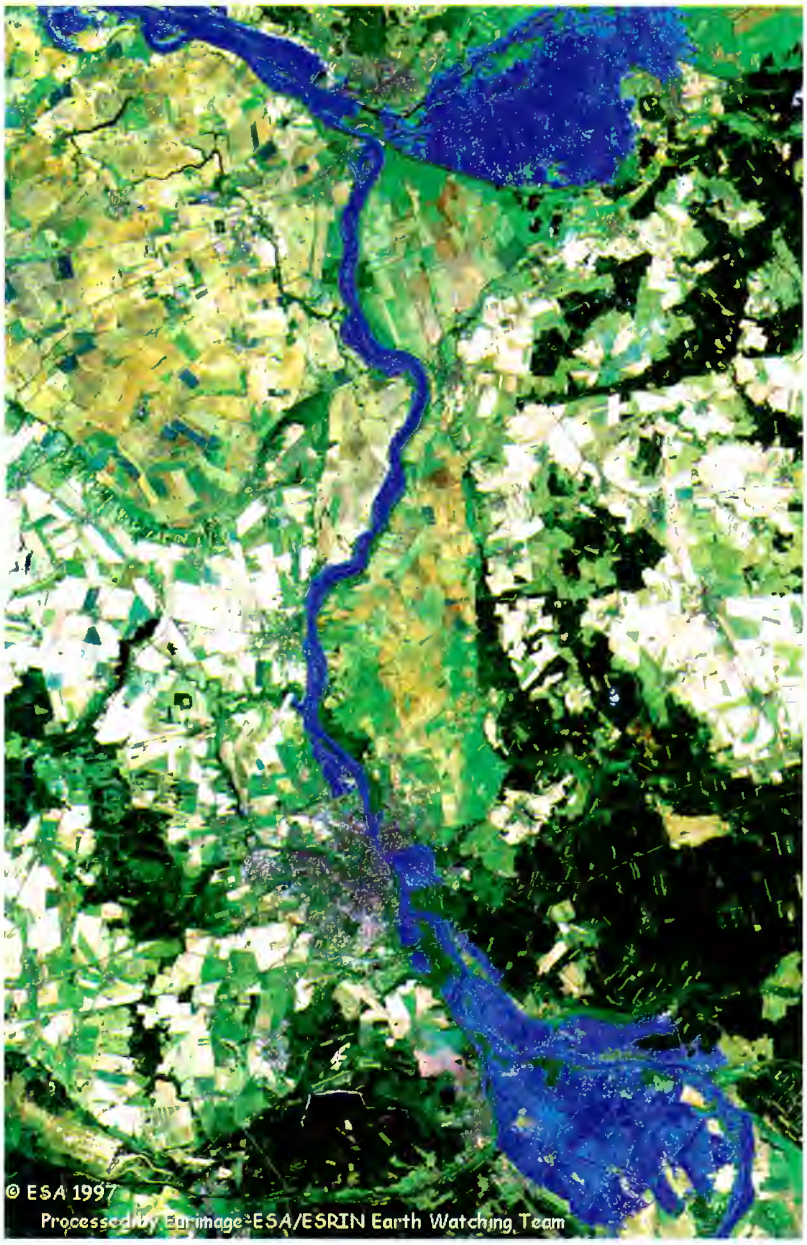

Frankfurt - Warta river area

This image is composed by superimposing a classification of an ERS multitemporal SAR onto a Landsat 5 TM (bands 752) image. The blue area (representing the flooding along the Oder and Warta rivers plain) was extracted from the classification of the ERS multitemporal image in order to better identify the damaged areas. The Landsat image provides the background in greater detail of the landscape, more similar to an aerial photograph or topographic map.This image is more easily interpreted, and it is valuable for land use mapping needed to estimate the damages amount for the different cultivations (e.g. for insurance company).

Landsat 752 acquired on 10/9/92 Classification of the ERS multitemporal SAR image (5/8/97, 6/8/97,28/5/97)

This image covers the upper part of the Oder river and, lower down, the Morava river valley on the left, showing the river swollen by the exceptional amount of water. The town of Opole is located near the upper center along the river. Due to cloudy weather it is very difficult to see the flooded areas, but some are visible near Wroclaw at the upper right corner. The town of Prostejov is hidden by the clouds just in the middle left. The confluence with the Svitava and Dyje river is located near the left border in the lower part of the image. It was not possible to acquire images over the Oder river because the weather was completely clouded. The towns of Brno, Wien and Bratislava are visible in the lower part of the image.

Floods - China, 1998

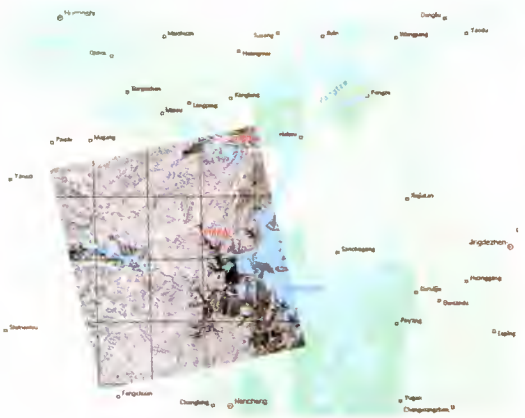

THESE OTHER TWO IMAGES, TAKEN BY THE ERS-2 SAR antenna, show a further two Chinese areas devastated by the waters.

Acknowledgement: ESA-MSTC China Co-operation Project involving the Ministry of Water Resources, China, and Remote Sensing Application Consultants, UK.

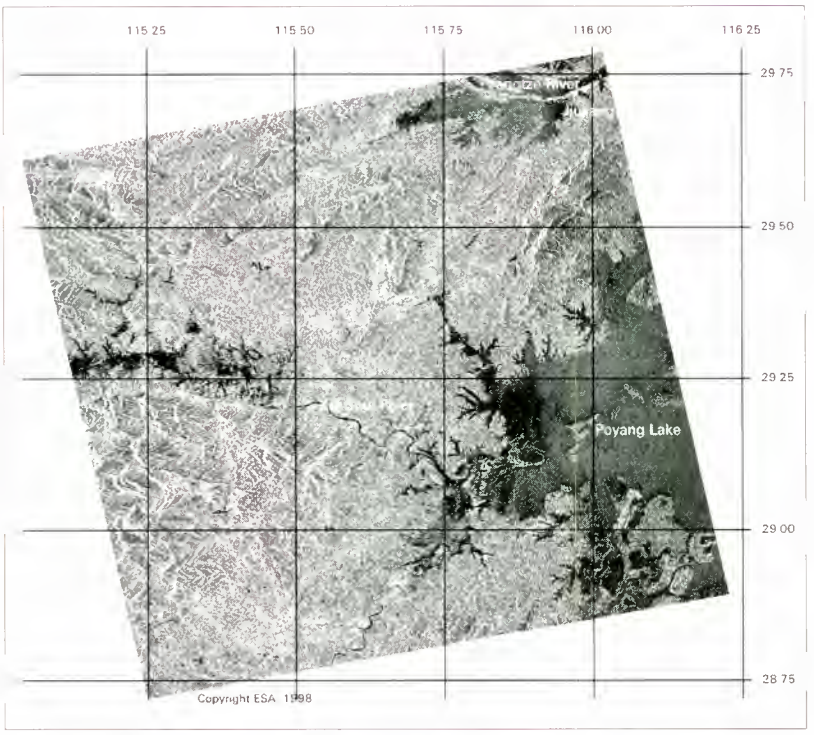

This ERS-2 SAR image (superimposed on a carthography in the upper image), centred around Yongxiu, North West of the town of Nanchang, was acquired by the satellite ground station of Beijing (China) on the 13th of August 1998 and processed within 12 hours from acquisition. The areas appearing in light blue (upper image) are those normally covered by water, namely by the Poyang lake on the right hand side of the image, by the Yangtze river in the upper right hand corner and by the enlargement of the Xiu Shui river on the left. The black areas correspond to areas that have been flooded by the above mentioned normal water bodies. Of particular relevance is the flooding in the western part of the Poyang lake that has largerly affected the flat territories North of Nanchang.

ERS-2 SAR image of the Nen river, Heilongjiang province, North East China acquired and processed by the Beijing Ground Receiving Station on the 5th of August 1998.

The flooded zone along the Nen river is 10-15 km wide over much of this section (in black in the image). Flooding seriously affected the important Daqing oilfields, with 255 oil wells being forced to close.

Map of the area

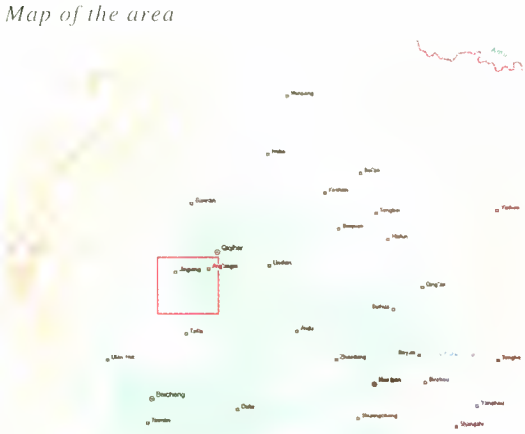

Floods - Yangtze, China, 1998

SEASONAL SUMMER RAINS have devastated larges areas of China this year, killing more than 2,000 people, destroying 2.9 million houses and ruining more than 9 million hectares of crops. Around the end of July torrential rains lashed central China causing the first several serious floodings. During the first week of August new rains in central Hubei and Hunan provinces pushed water levels on the upper reaches of the Yangtze to a third flood peak, and hit Hubei's provincial capital Wuhan where water levels have risen to 1.25 meters above danger levels also cutting power supplies.

Floodwaters washed away a 3,000 meter section of newly constructed dikes in Hunan's Huarong County (see images below) and opened a 600 meter crack in the embankment surrounding Caisang Lake, both near Yueyang. Officials said that floods, landslides and mudflows have affected some 240 million people - one-fifth of China's population.

This ERS-2 SAR image, centred between Huarong (200 km Southwest of Wuhan) and the Yangtze River, was acquired by the station of Ulan Bator (Mongolia) on the 1st of August 1998. The areas in black are those covered by water during the satellite pass. To discriminate the flooded areas from the normal rivers flow, a semi-transparent layer with the rivers in light blue was superimposed. The portion covered by water of the area near Huarong (in gray instead of black due to wind conditions) below the dikes (on the right edge near the mid-bottom of the SAR image) is more than doubled.

ERS-2 SAR
Orbit 17149
Frames 2997 & 3015
Acquired by
Ulan Bator Station

Floods - Belgium, 1998

TORRENTIAL RAINS in mid September over Belgium and the Netherlands caused heavy flooding of some regions and vast soil moisture.

Data acquired by ERS-2 SAR over Belgium on September 16th (orbit 17812), a couple of days after the main event, was received in near real-time by the Earth Watching Team and combined, in a multitemporal image, with ERS-2 data from previous August acquisition (orbit 16100).

In this multitemporal image, the city of Bruxelles appears as a large, very bright area near the center, with the black shape of its airport in the North-East.

All the blue spots clearly show the effects of the heavy rainfalls on cultivated areas, which are still moist.

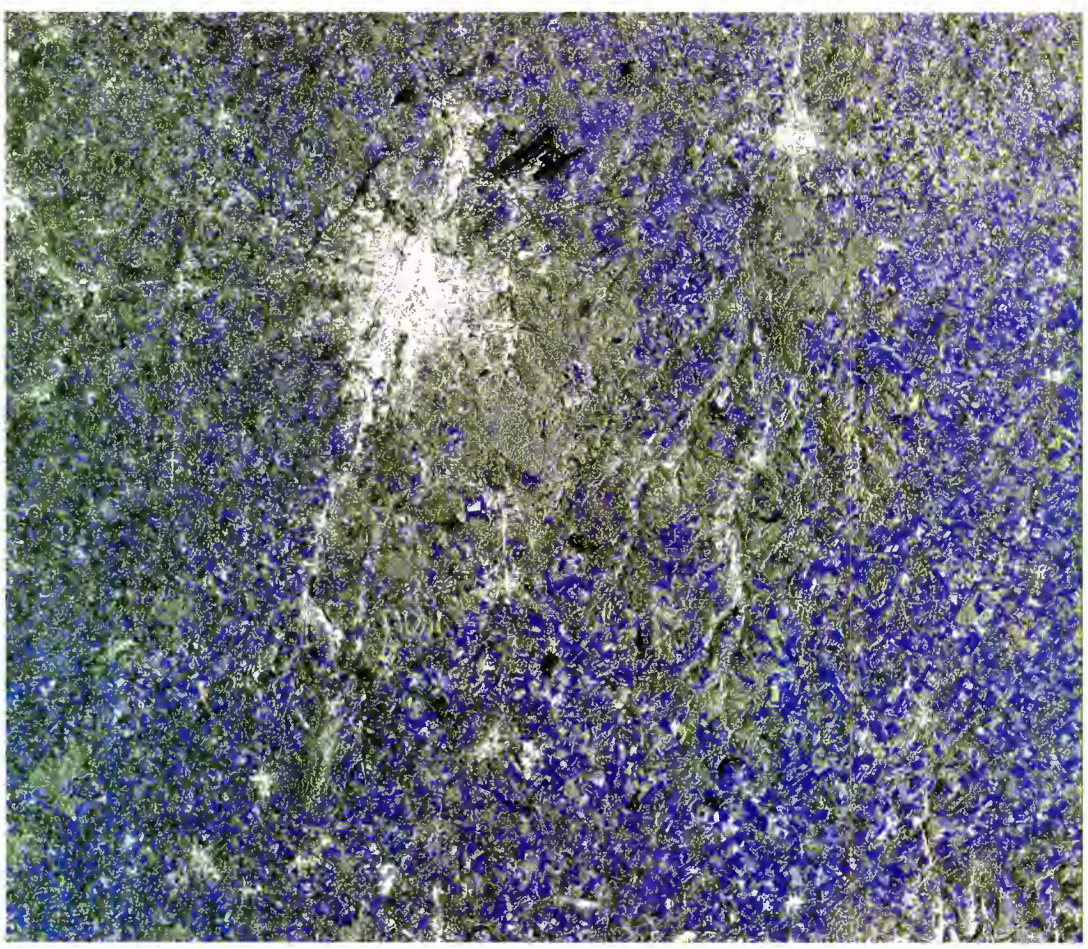

ERS-2 SAR multitemporal image
Orbits 16100 & 17812
Frame 2565
Area covered: 70 x 70 km

Floods – Mitch - Honduras, 1998

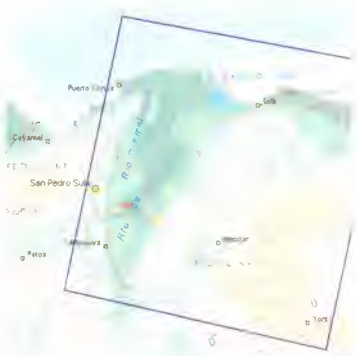

THE CYCLONE MITCH has devastated parts of Honduras, Nicaragua, El Salvador and Guatemala, becoming the most destructive Atlantic storm since the Great Hurricane of 1780, blamed for 22,000 deaths in the Eastern Caribbean.

The death toll in Honduras has risen to almost 10,000 people, another 1 million are homeless. In Nicaragua 20 percent of the population are homeless and it will cost an estimated $1 billion, half the nation's annual economic output, to rebuild what was destroyed.

The storm's impact on key exports — including coffee, bananas, sugar and peanuts — threatens to set the region's economy back of decades, a hardship that will spread to consumers around the world. It has been estimated that 70 percent of the nation's economic output has been lost.

MITCH formed in the Southwest Caribbean Sea, from a tropical wave, about 360 miles South of Kingston, Jamaica late on the 21st of October. The system initially moved slowly Westward and intensified to a tropical storm. Mitch then moved Northward, then Northwestward on the 23rd and 24th and gradually gained strength. On the 24th it turned West and became a hurricane.

The central pressure reached a minimum of 905 millibar about 40 miles Southeast of Swan Island on the afternoon of the 26th. This pressure is the fourth lowest ever recorded, in an Atlantic hurricane, during this century.

ERS-2 SAR Multitemporal image acquired on the 5th of November 1998 and on the 16th of October 1997. The flooded areas along the Olua river are clearly shown in blue

At its peak intensity, Mitch's maximum 1-minute sustained surface winds were estimated to be 320 km/h. The cyclone center passed very near the Guanaja Island and then, up to the 29th near the North coast of Honduras. The 5th November, Mitch became extra-tropical and it dissipated on the North Atlantic Ocean.

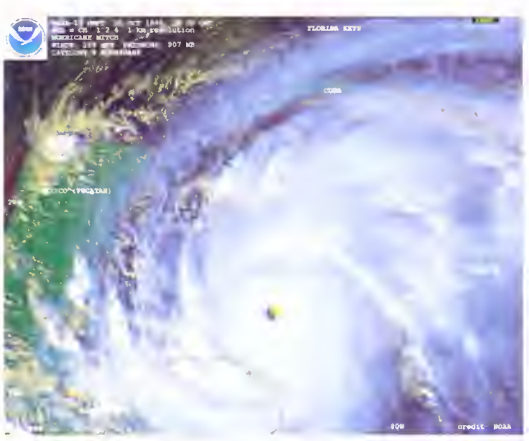

NOAA image acquired on the 26th of October

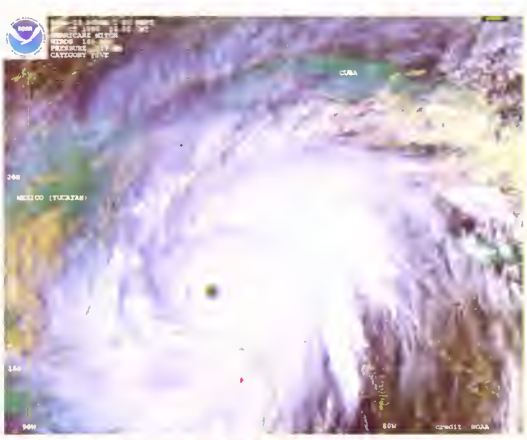

NOAA image acquired on the 27th of October

Mozambique Flooding 2000

The blue frame show the coverage of the below ERS-2 SAR mosaic around the town of Xai-Xai

The ERS-2 Satellite passed over the Xai-Xai area on the 16th of March while the flooding was still present. Combining this image with an previous one (27th of March 1997), a multitemporal mosaic (right image) has been generated highlingting the flooded areas (in blue). The towns of Chibuto and Xai-Xai are visible as a cluster of bright yellowish points.

To better show the difference with respect to the normal situation, a map was superimposed on the mosaic: the flood exstension versus the normal situation (light blue) is evident.

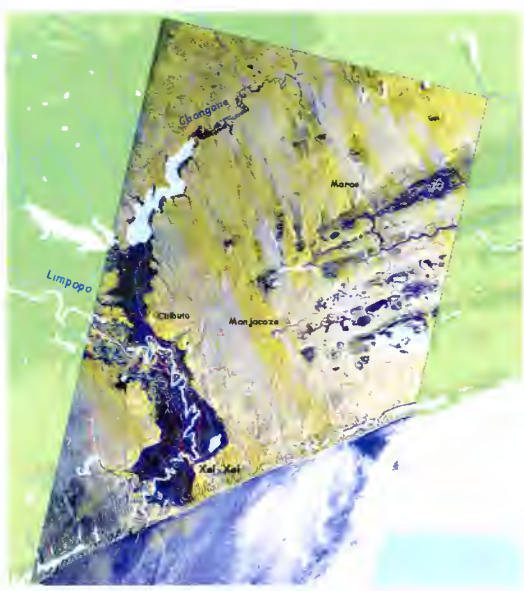

Cyclone Eline hit Mozambique on Tuesday 22 February, ripping roofs off houses, washing out roads and stranding thousands of residents. Even before the storm hit, weeks of flooding had killed scores of people and displaced more than 200,000. The center of Eline skirted the main towns of Mozambique leaving vast stretches of land submerged under muddy brown water and accessible only by air. Despite several years of economic growth, since a 15-year civil war ended in 1992, Mozambique remains one of the poorest countries in the world. The bulk of its 19 million people lives in huts, earns less than a dollar a day and has no access to basic services. The floods have washed away many crops, making the situation even worse.

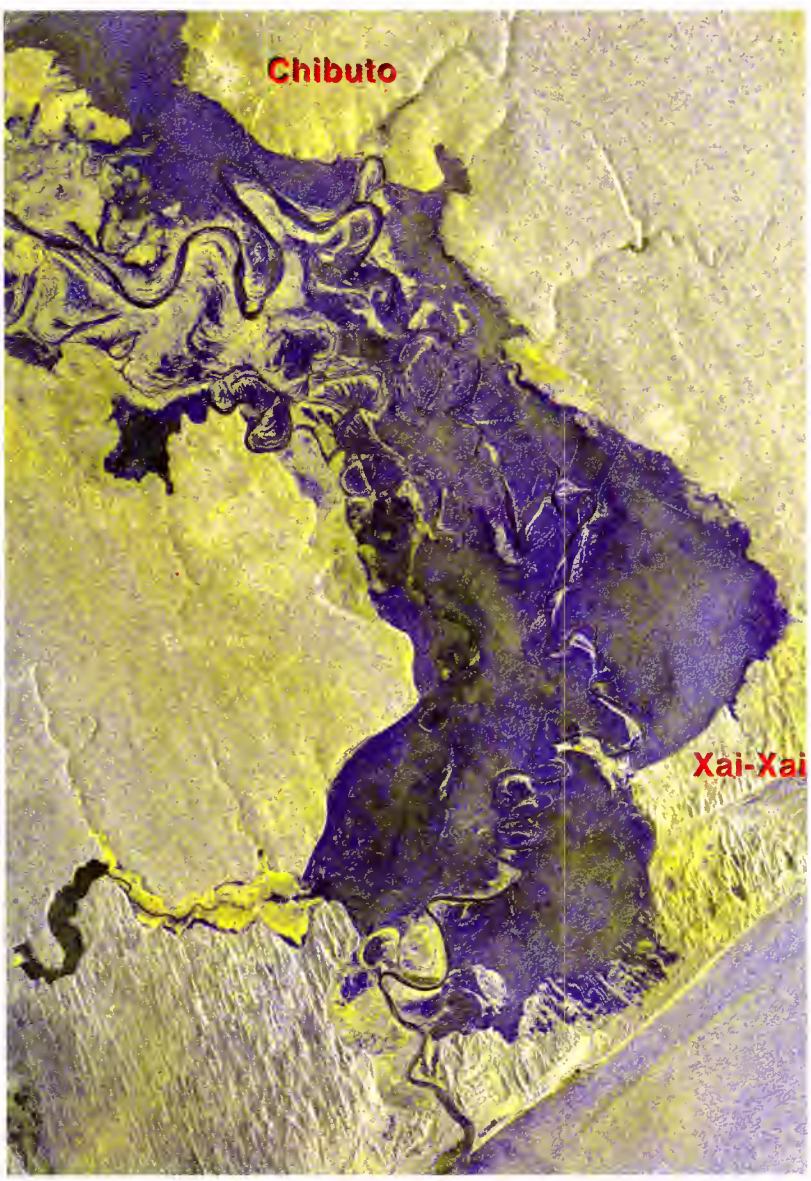

ERS-2 SAR Multitemporal
Orbits: 10109 & 25640
Dates: 27/3/1997, 16/3/2000
Frames: 4095, 4113
Acquired by:
Johannesburg Station

ERS-2 SAR
Frame 4113
Acquired by
Johannesburg Station

Oil Spills

EACH YEAR SHIPS AND INDUSTRIES damage the delicate coastal ecosystem in many parts of the world by releasing oil or pollutants into rivers and coastal waters.Off-shore environments are also polluted by mineral oil mainly due to:

- tanker accidents, when large amounts of oil are spilled into the sea
- illegal oil discharges by ships during "normal operations"
- natural oil seepage

After a tanker accident the biggest problems is to obtain an overall view of the phenomenon, getting a clear idea of the extent of the slick and, if possible, predicting the way it will move. For natural and man-made oil spills it is necessary to operate a regular monitoring program. Aerial surveys over large areas (e.g. the Mediterranean Sea) to check for the presence of oil are limited to the daylight hours in good weather conditions. The Mediterranean Sea has extensive marine traffic because it gives maritime access to the Middle East (and the Suez Canal), the Black Sea and Southern Europe; much of this traffic is oil tankers. The result of this high level of traffic is a high risk of pollution and even ecological disaster, made worse by the fact that it is a closed sea.

Oil pollution monitoring in the Mediterranean Sea is normally carried out by aircraft or ships. This is expensive and is constrained by the limited availability of resources. Satellite imagery can help greatly in this field, identifying probable spills over very large areas and then guiding aerial surveys for precise observation of specific locations. The Synthetic Aperture Radar (SAR) instrument, which can collect data independently of weather and light conditions, is an excellent tool to monitor and detect oil on water surfaces. This instrument offers the most effective means of monitoring oil pollution: oil slicks appear as dark patches on SAR images because of the damping effect of the oil on the backscattered signals from the radar instrument. This type of instrument is currently on board the European Space Agency's ERS-1 and ERS-2 satellites, on the Japanese JERS-1 satellite and on the Canadian Radarsat satellite. In the future more satellites, such as ESA's Envisat, will carry SAR.

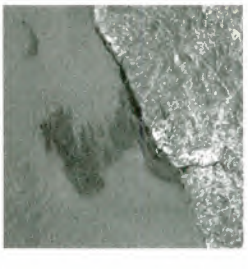

Oil Spill – Strait of Tunis

This image, part of a series of SAR acquisitions over the strait of Tunis, was used to detect oil spills in a high-traffic region of the Mediterranean sea. A number of ships were detected (marked by red circles in the image) and some oil spills found with high and medium probability. The idea was to cooperate with the Italian Coastguard to improve controls on pollution. From an image like this one, it is possible to extract only the useful information (like the coloured signs), add a geographical grid and send only this information to the ships via fax.

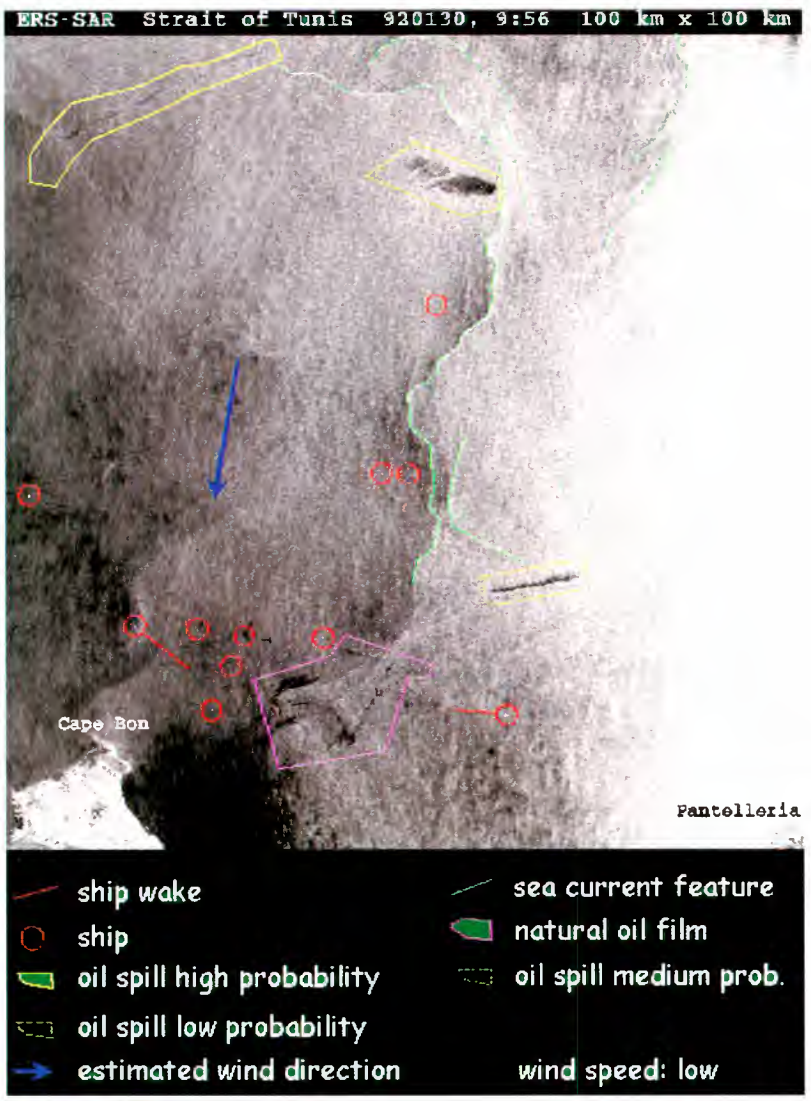

Oil Spill – Portugal, 1994

OPORTO, PORTUGAL. On the 2nd October 1994 the Panamanian oil tanker Cercal struck a rock while entering the harbour of Leixoes (the Oporto harbour), releasing about 1.000 tonnes of crude oil into the sea.

ERS-1 SAR
4 October, 1994
Orbit: 16838
Frame 2781
Acquired by Fucino (Italy)

The ESA ERS-1 satellite acquired this SAR image two days after the accident. Because of the damping effect of the oil, the reduced roughness of the sea surface appears clearly as a black mark on the SAR image. The spill can be seen floating along the coast and out into the sea. The coastal city of Oporto, lying near the centre of the oil spill, appears as a cluster of white dots. The rainy and foggy weather that prevailed in that region of Portugal on the date of the accident made it very difficult to evaluate the spill from an aircraft. However, thanks to the all-weather capabilities of the ERS-1 SAR instrument it was possible to acquire this very useful scene through the cloud cover.

Oil Spill – North Sea, 1996

THE SCENE WAS ACQUIRED from the European Space Agency's ERS-2 satellite on July 18 1996, at 11 AM (Greenewich time) by the Fucino ground station, but also by Tromso Satellite Station (TSS). The Earth Watching Team discovered during a data screening some oil slicks in this image and asked the expert-operators of TSS for an interpretation.

The overall low grey level in the scene suggests that there is little wind in the area, with a range of from about 1m/s to 7m/s. These are ideal conditions for detecting any type of oil films. In the image, located northwest of Bergen (Norway), there are two possible oil slicks of mean sizes 12 x 5 km and 14 x 3 km. Both slicks are diffuse and it looks like the wind has worked on them. They are probably several hours old. Due to the optimal conditions to detect surface dumping features, slicks in connection with almost every oil platform (very bright points) in the image can be observed. These slicks may be caused by water disposals, drilling fluids or oil. The almost completely black area at Northeast of the image is due to low wind conditions.

Operators at the TSS are routinely analysing all SAR data received at the station. If an oil slick is discovered, as in this case, a communication is sent to the Norwegian Pollution Control Autority (SFT) by phone and fax. The surveillance aircraft of SFT often operates in the vicinity of the satellite acquisitions and a direct link between the operators of TSS and the pilots has been established.

ERS-2 SAR
July 18th, 1996

Volcanoes

Volcanic activity, both past and present, is subject to constant study and analysis in the search for improved land-use planning, the scope of which is to help minimise hazard in risk areas.

Authorities often need data over volcanic areas, not only to monitor eruptions, but also to produce maps and thematic diagrams predicting the potential risk to the surrounding area.

In this field, remote sensing data is used to detect lithological differences, vegetation changes, altimetric variations after volcanic events, and the extent and growth of urban areas into endangered areas.

In addition, satellite data can provide an overview of large volcanic areas in a single frame, making it possible to create image maps of areas as large as 180 x 180 km, with an accuracy comparable to 1:100000 map scale from a single Landsat 5 TM pass over the area. A higher resolution can be achieved by taking data acquired by other satellites (KVR, SPOT, IRS, etc.) and merging these high resolution images with Landsat or other multispectral sources.

The study of volcanic areas is mainly done from optical data, so that the same ground target can be examined in different spectral bands (usually ranging from visible to far infrared).

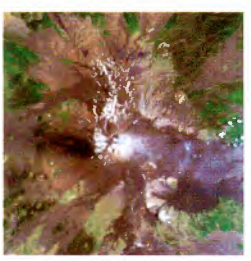

Radar missions such as the European Space Agency's ERS satellites, make a unique contribution when the need is for altimetric change detection, or when volcanic eruptions cause other phenomena that can be monitored by radar sensors (lava flow, ground fissures, earthquakes, mud slides, floods, etc.).

The following pages show photos, ground information and satellite images to help in the interpretation of the remote sensing data for the analysis of features not detectable on photographs.

Vatnojakull Eruption & Flood

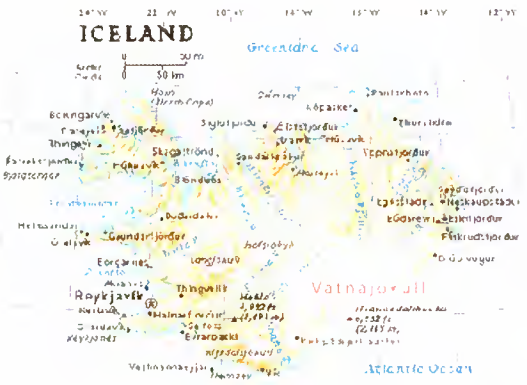

Late on the evening of September 30, 1996 an eruption started beneath the Vatnajokull glacier in central Iceland. The glacier was being melted by the heat from a 4km fissure under the ice.

By October 14th, the eruption was effectively over, but the trapped meltwater had raised the level of the Grimsvîtn lake by some 100 m by the time it eventually broke out to the south, causing devastating floods in the Skeidarasandur region before draining into the Atlantic Ocean.

The map below shows the affected regions. The map was scanned from aeronautical maps of the area and shows elevations in feet - divide by three to get a rough equivalent in metres. The Vatnajokull glacier is the largest glacier in Iceland, covering more than 10,000 square km. The smaller rectangle marked on the map shows the approximate location of the volcanic event, and measures about 20 x 20 km. Click inside the rectangle for an account of the eruption. The larger rectangle shows the approximate location of the flooding, and measures about 60 x 70 km.

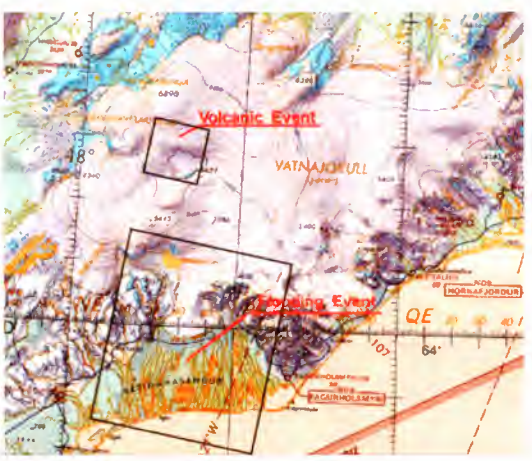

The Eruption

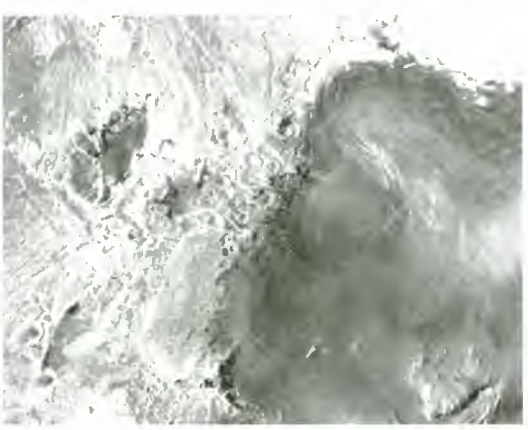

This SAR image was acquired from the European Space Agency's ERS-2 satellite on September 1, 1996, a month before the event. It shows the normal scene on the glacier. The crevasse that lies between Mounts Svianukar and Grimsvîtn is clearly visible in the Southeast corner, while the ridge of Mount Grimsvîtn is just visible at the surface of the ice to the Northwest. Apart from these features and two other ice features in the west of the image there is no sign of anything but the smooth, wet surface of the snow-covered ice cap.

Late on the evening of September 30, 1996 an eruption started beneath the glacier. Over the previous 24 hours a sequence of earthquakes had been recorded around the Bardarbunga caldera. Similar earthquakes have occurred beneath the volcano many times during the last 22 years, but none had significant aftershocks, or were followed by magmatic activity such as this last earthquake. Numerous quakes, including 5 with magnitude over 3, were recorded in two hours. Shortly after 1300 hours Science Institute seismologists informed the Civil Defence authorities as well as the scientific community of this unusual seismic activity and the possibility of impending eruptive activity.

Vatnojakull Eruption & Flood

The eruption site was discovered early Tuesday morning (Oct. 1) from an aircraft. By that time two elongated, 1-2 km wide subsidence cauldrons had formed on the ice surface of Bardarbunga, on the northern flank of the neighbouring Grimsvîtn volcano. The cauldron formation indicated that the glacier was being melted by an eruption on a 4 km long fissure beneath the glacier, which is 400-600 m thick here. The meltwater drained into the Grimsvîtn caldera under the ice shelf of the lake. In less than 24 hours a third of a cubic km of water had been added to the lake. By October 2 one of the active craters had melted its way through the glacier and a massive steam column rose from the cauldron up to an elevation of 10.000 meters.

This image, acquired by Kiruna station just 4 days after the eruption began, shows how the heat has broken through the surface of the ice. An irregular white line represents the steep slopes of a canyon formed by ice melting. At the top of this line the black streak towards the north shows meltwater on the top of the ice.

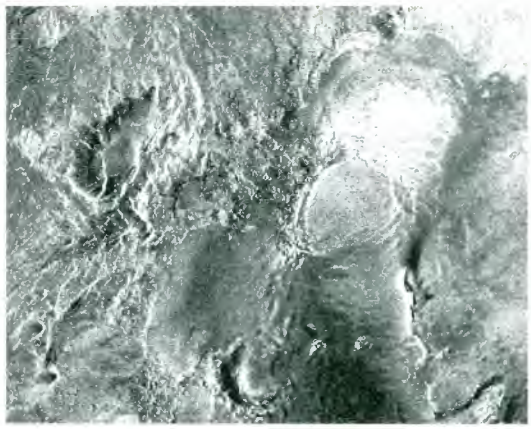

By October 9 the eruption was taking place on a 9 km long fissure and volcanic products piled up above the fissure forming a mountain ridge which in places approached 200 m high. About half of the area of Vatnajokull was covered by a thin layer of ash.

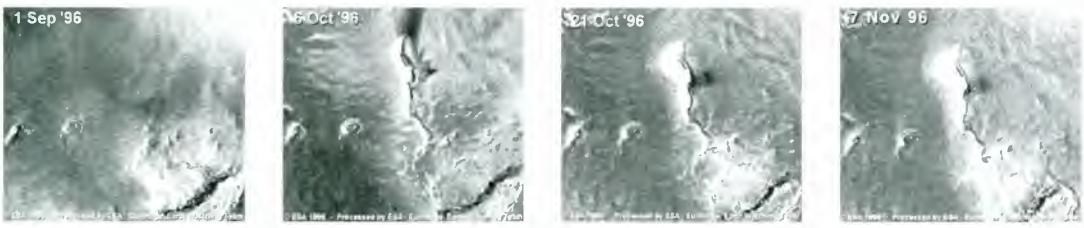

This image sequence shows the evolution over the area where the fissure appeared. The similarity of the image acquired on October 21 (by the ERS-1 satellite), with that of 7 November, show that by these dates the eruption was over. The dark streak of meltwater is no longer present. The trapped water is breaking out to the south-west of this point, causing catastrophic floods. Another image, acquired on the 22 October by ERS-2, has been used to create interferograms to reveal the full scale of the topography changes.

Interferometry results

Intensity *Obtained by summing the intensity values of the two images. Due to the very short timeframe between the two acquisitions, the result is quite similar to the intensity of one acquisition only.*

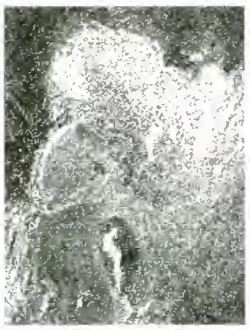

Coherence *Obtained comparing the two images in intensity and in phase. In this way it is possible to detect very small changes. The dark areas indicate low coherence where the changes occurred.*

Phases *The phase difference between the two images. Each gray cycle (from black –0°– to white –360°) represents a height difference. Due to this phase repetitivity several cycles are visible.*

Unwrapped phases *Obtained from the previous one by adding 360° several times, to unwrap the phases. Dark blue indicates the lower parts of the image, while red the higher ones. The phase values are converted to altitude values.*

The ERS radar satellites have also another capability: through the technique of interferometry, they can detect land movement and build 3-dimensional images from a pair of images. Thanks to the availability of 2 satellites, ERS-1 and ERS-2, with only one day's difference (the interferometric results shown here have been obtained with the tandem pair acquired on the days ofthe 21st and 22nd of October) can measure the event with great precision. For interferometry the data used include the phase values, that is omitted from the standard product (PRI).

Since the data was acquired only one day apart, a reasonably good coherence over the whole scene is present, with the exception of a pear-shaded area around the fissure. This area was still subject to strong vertical and horizontal movements between the acquisitions, which make the data acquired in successive days uncorrelated for the retrieval of any reliable phase information.

The images at left show an area of approximately 36 km per 44 km around the eruption site.

The area around the fissure can be easily detected as the low coherence pear-shaded region, at the bottom-center part of the coherence image. This lack of coherence is translated in a completely noisy area in the interferometric phase image. The quality of the applied unwrapping is appreciated on the unwrapped phase map, since errors due to lack of coherence are not propagated outside the low coherence region.

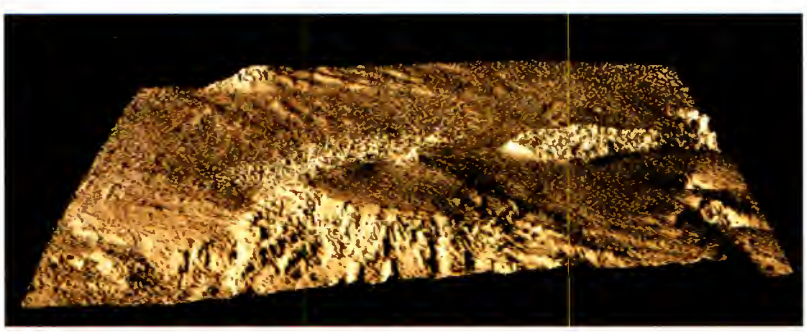

3 dimensional image obtained from the unwrapped data (of a larger area than the image at left). It shows where the terrain is still moving.

The Flood

The Jîkulhlaup. or glacial flood, is a regular feature of this area. Earliest accounts date back to the 12th century, and large Jîkulhlaups have been recurring every 5 – 15 years since 1900 – but the flood of November 1996 was to be the most catastrophic since 1938. This map clearly indicates the area of glacial runoff between the Vatnajokull and the Atlantic Ocean. It is an area about 20 - 30 km wide.

During the JIikulhlaup, icebergs broken off the glacier were carried down on the flood, sweeping away several of the bridges across the river, the water in the caldera fell 165 m, and up to 100 million tons of volcanic material and clay were carried out to sea as far as 15 km from the coast. The plain was strewn with icebergs weighing up to 1000 tons

The level of water in the Grìmsv–tn caldera had sunk to 1330 m after a J–kulhlaup in April of that year. After the eruption an enormous quantity of water continued to pour into the lake. By October 10 it had risen to 1485 m. Two days later a GPS instrument was placed on the ice, allowing continuous and exact measurements. By the next day the level was 1500 m, increasing at the rate of 25 cm per day. The Jîkulhlaup normally begins when the level reaches 1430 m, with the water finding its way slowly through the ice. At over 1510 m the water pressure was sufficient to lift the glacier ice off the ground, causing the sudden runoff of the water underneath. Icelandic scientists were preparing for some 4.5 km3 of water to strike Skeidarasandur.

Using the BDDN (Broad Data Dissemination Network) system. it was possible to obtain the images from the receiving station of Kiruna (Sweden) in real-time. Thus the images were processed while the event was happening. and put on-line on Internet within one day.

This image was acquired on 22 October, before the floods burst out, and shows the normal situation. It is clearly an area of high water flow, but the image suggests a pattern of deposition from the meltwater outflows, leaving the coarser deposits with their higher backscatter close to the glacier, while towards the sea are smooth beds of finer gravel and sand

This image, acquired on 7 November, shows the difference after the flood. Backscatter remains high, from the mouths of the meltwater streams all the way to the coast, indicating that a large quantity of coarse material has been deposited. The rivers in the main are too turbulent to give the normal low backscatter associated with river water.

Tropical Cyclones

Tropical Cyclones derive their energy primarily from evaporation of the sea, in the presence of high winds and lowered surface pressure, and the associated condensation in convective clouds concentrated near their center. Every year Tropical Cyclones produce important damages on a high number of countries. The floods caused by the heavy rain, strong winds and bad sea conditions produce huge human and economic losses. Nearly 100 Tropical Cyclones occur each year on seven regions around the world called 'basins'.

Tropical Cyclones are individually named to provide ease of communication between forecasters and the general public regarding forecasts, alertness and warnings. Since the storms can often last a week or longer and more than one Cyclone can occur in the same basin at the same time, names can reduce the confusion about the storm being described. A strong Tropical Cyclone is also called hurricane in the United States and in the Caribbean (when the wind speed is greater than 33 m/s) and typhoon in the West of the Pacific Ocean.Wind observations over Oceans are largely made by merchant ships. However, ships' reports are sparse and inadequate, particularly for storms. The spatial resolution of numerical analysis performed by weather forecast centers are generally insufficient to reveal accurate position and details of the Cyclone.

Satellite visible and infrared images may help to locate storms but do not reveal the surface intensity. Only an active microwave sensor, the Wind Scatterometer, has the proven capability of measuring both wind speed and direction under the widest range of conditions with high spatial resolution (*).

Since the launch of ERS-1 in 1991, the Wind Scatterometer's derived wind-fields, together with wave height measurements from its Radar Altimeter and wave spectra data, have been continuously provided, within 3 hours of measurement time, to national and international meteorological and oceanographic organizations, via the Global Telecommunications Service of the World Meteorological Organization, to improve regional and global meteorological and metocean forecasting and nowcasting services.

The purpose of the Wind Scatterometer is to obtain information on wind speed and direction at the sea surface. It operates by detecting the change in radar reflectivity of the sea due to the perturbation of small ripples by the wind close to the surface.

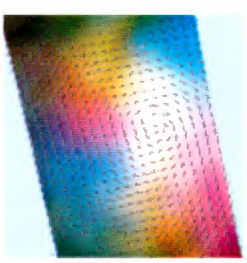

The information on the atmospheric structure derived from the wind-field, observed by the Wind Scatterometer, allows relocation of low pressure regions, in some cases by as much as several hundred kilometers, with considerable impact on the accuracy of short and medium terms forecast.

The Wind Scatterometer therefore provides not only a large amount of wind measurements of homogeneous quality to the meteorologists, but moreover it supplies detailed information on very intense structures such as Tropical Cyclones, for which it is normally very difficult to obtain high quality measurements.

(*) (Liu and Tang)

Cyclones - Yali, 1998

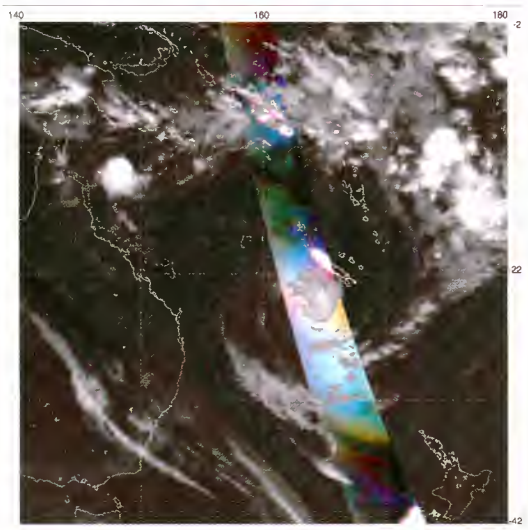

ERS-2 Wind Scatterometer image superimposed on a GMS metereological image of the 24th of March at 11.32 UTC

YALI SPENT MOST OF ITS LIFE in the Fiji area. It moved westwards across the 160 East meridian on the 25th of March to the Australian region for a couple of days before undergoing rapid deepening as an extratropical cyclone and pommelling New Zealand with fast winds, high sea waves and heavy rains.

The images show data from the Wind Scatterometer instrument coloured in red, green or blue according to which of the three antennas of the instrument provided the measurements. Each antenna provides a measure of the sea surface roughness from a particular viewing angle and this can be related to the speed and direction characteristics of the local windfield. In general, the measured sea surface roughnesses from each antenna are combined into a standard wind field product which provides accurate wind speed and direction measurements over an area of approximately 500 by 500 km with a grid spacing of 25 km.

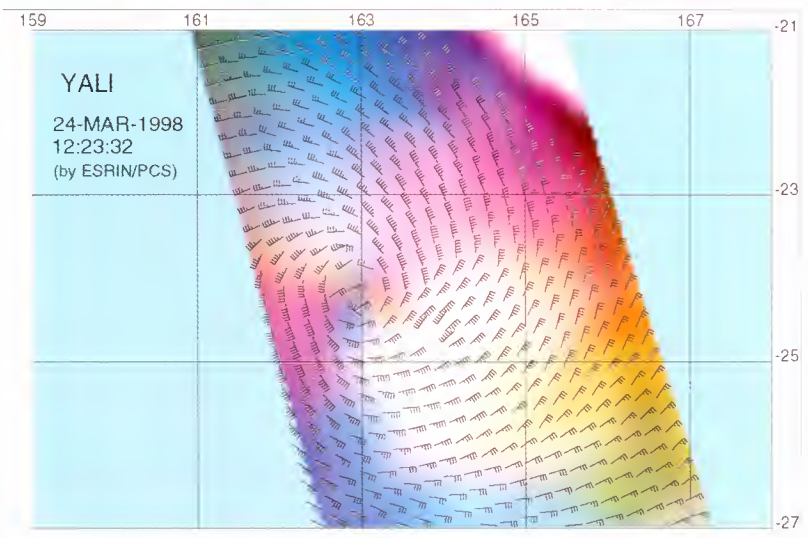

ERS-2 Wind Scatterometer image of the 24th of March 1998 at 12.23 UTC

Regarding the temporal resolution, the satellite is able to obtain an image of one Tropical Cyclone every 24-48 hours. The image shows a representation of the tropical cyclone Yali which lived in the Pacific Ocean from the 17th to the 27th of March 1998 based on measurements of the Wind Scatterometer instrument. The maximum wind speed measured in this image is 55 Kts.

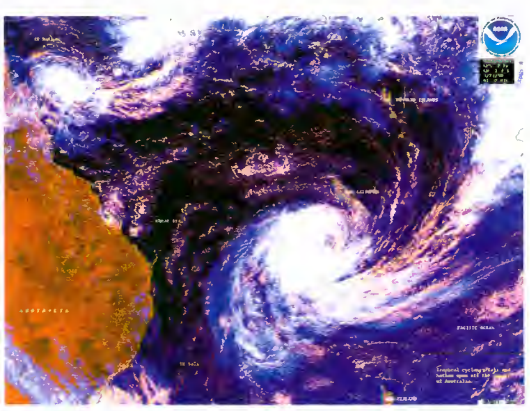

GMS satellite image of the 24th of March 1998 at 1.32 UTC

Two days later GMS takes this image at 1.32 UTC

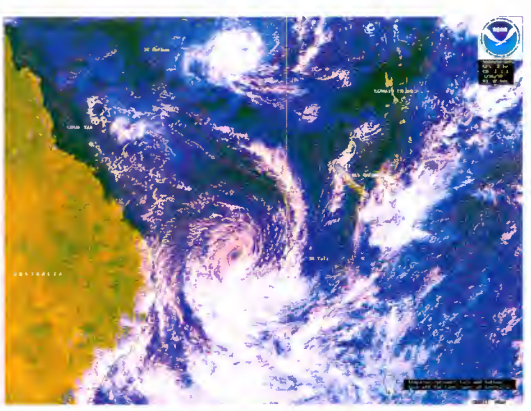

Cyclones - Danielle, 1998

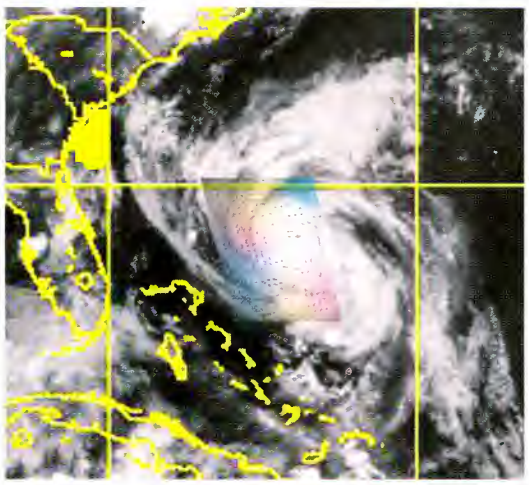

ERS-2 Wind Scatterometer image superimposed on a GOES-8 metereological image of the 31st of August at 3.15 UTC

DURING THE LIFETIME OF DANIELLE, wind speeds greater than 100 Kts were recorded. Danielle formed over the central tropical Atlantic ocean on the 24th of August becoming a tropical storm later that afternoon. Danielle reached hurricane status on the 25th and moved on a West-NorthWest track for the next 5 days. At the moment of this image, Danielle was near Florida, but on the next days begun to move to the North and North-East following the East coast of the United States and Canada and turning to the East until it became extratropical on the 4th of September at latitude 40 North-West.

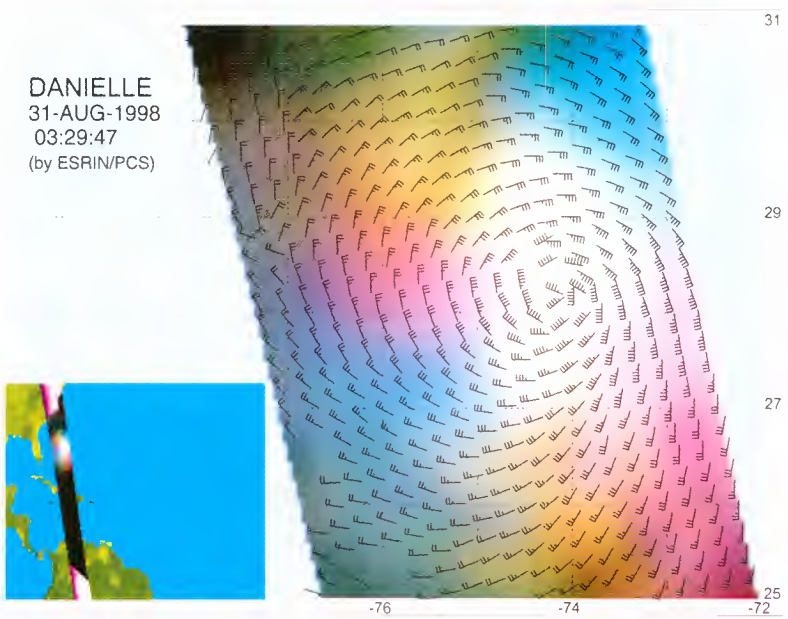

This image shows a representation of the tropical cyclone Danielle (which occurred in the Atlantic Ocean from 24th of August to 4th of September 1998) taken on the 31st of August at 3.29 UTC and based on measurements obtained by the Wind Scatterometer instrument. The maximum wind speed measured in this image is 80 Kts.

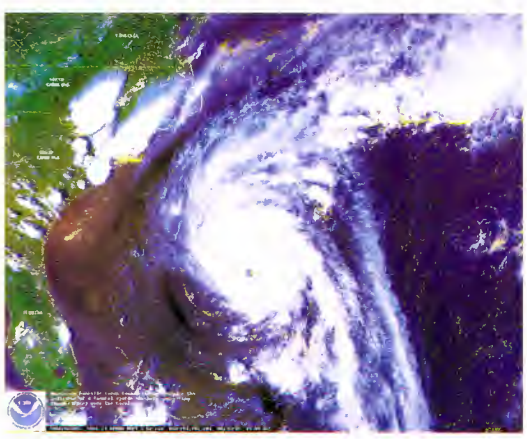

NOAA 14 AVHRR image of the 31st of August, 1998 at 19.08 UTC

As it can well be seen on the images the tropical cyclones are characterized by a thermal circulation containing a spiral convergence of warm air toward the center of the system at low levels, and a region of ascending air close to the center surrounded by a descending region. The air diverges at the top. The generation and maintenance of the warm zone close to the center results from the heating and humidification of the convergent air of the low levels by flows of water vapor, sensible heat coming from the surface of the sea above which it flows, and the release of latent heat associated with the very thick vigorous convection in the convective ring surrounding the eye of the cyclone and in the spiral bands.

Earthquakes - Turkey 1999

A STRONG EARTHQUAKE shook Northwestern Turkey early Tuesday 17th of August, levelling buildings, cutting power and phone lines and sending frightened residents into the streets. The National Earthquake Information Center, said the quake had a magnitude of 7.8 Richter, making it nearly as powerful as the 7.9 magnitude of San Francisco's earthquake, which killed 700 people in 1906.

The earthquake's epicenter was between Izmit and Bursa, some 100 km East of Istanbul. Casualties were reported as been high in the nearby towns of Golcuk, Derince and Darica. A fire broke out at an oil refinery near Izmit, an industrial city of 500,000 people. Another large city badly affected by the earthquake was Adapazari, located North-East from the Sapanca Lake.

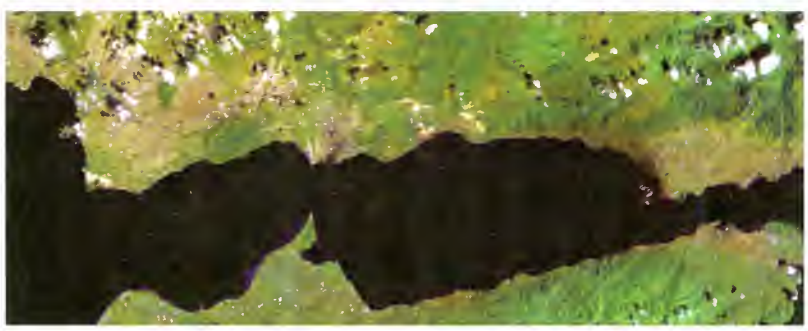

Landsat 7 ETM+ image of the 17th of August

The death toll rose by the hour as more debris was removed and contact with several towns and villages, cut off by earthquake damage, was re-established. On the 18th, while rescuers frantically scraped through the debris, fire-fighters battled a raging fire at Turkey's largest oil refinery at Derince. Aircraft dropped chemical flame retardant on the blaze, which threatened to consume the entire facility. Officials feared an explosion if the fire was not contained soon.

Four days after the 7.4 earthquake struck, the Turkish Crisis Center in Ankara said the death toll had risen to 10,059 and government sources told a Turkish newspaper they feared the death toll could rise to 20,000. More than 45,000 were injured and thousands were still missing.

Landsat 5 TM image of the 18th of August

The images show clearly the fires which resulted from the earthquake: the major one in the rafinery of Derince. Small fires are also visible as gold-reddish points in the images of the 17th and 18th . Another phenomenum, well highlighted in the bottom right image, is the bradyseism movements apparent along the coast near the harbour of Golcuk (see red arrows). Whilst the large blue area, in the same image around Derince, represents the smoke of the refinery fire.

Detail of the above image showing the refinery on fire

Multitemporal Landsat 7 Panchromatic image showing the differences between the 10th (before the event) and the 17 of August (after the event)

Stabilimento Tipolitografico Ugo Quintily S.p.A.
Viale Enrico Ortolani, 149-151 – 00125 Roma – Tel. 06.52.69.285
Finito di stampare nel mese di novembre 2000

For Further Information:

on ESA's Remote Sensing missions or applications, contact:

EOHelp
ESA-ESRIN
Via Galileo Galilei,
00044 Frascati, (Rome) Italy
Tel. (+39) 06 94180 777
Fax (+39) 06 94180 272
E-mail: eohelp@esa.int